PARTIAL OXIDATION OF O-XYLENE IN A TRANSPORTED-BED REACTOR

THE PARTIAL OXIDATION OF ORTHO-XYLENE IN A TRANSPORTED-BED REACTOR

By

THEODORE REGINALD PAETKAU, B.Sc. (ENG.)

A Thesis

Submitted to the Faculty of Graduate Studies

in Partial Fulfilment of the Requirements

for the Degree

Master of Engineering

McMaster University

October 1966

MASTER OF ENGINEERING
(Chemical Engineering)

McMASTER UNIVERSITY
Hamilton, Ontario.

TITLE: The Partial Oxidation of Ortho-Xylene in a Transported-Bed Reactor

AUTHOR: Theodore Reginald Paetkau, B.Sc. (ENG.) (University of Alberta)

SUPERVISOR: Professor T. W. Hoffman

NUMBER OF PAGES: (ix), 122

SCOPE AND CONTENTS:

The partial, catalytic oxidation of ortho-xylene was investigated in a transported-bed reactor in which the vanadium pentoxide catalyst in the form of extremely small particles (average particle size of 45 microns) was conveyed upward by the reacting gases.

The reaction was studied at a contact time of about 0.2 seconds, at air-to-o-xylene molar ratios of 42 to 86, at catalyst-to-gas ratios of 8 to 23, and at a reaction temperature of 750°F (400°C).

Reaction products were analyzed by Gas Chromatography and Nuclear Magnetic Resonance Spectroscopy.

Product analysis indicated a high yield of o-tolualdehyde, small yields of other oxidation products, but only trace amounts of phthalic anhydride. These results are consistent with proposed mechanisms for this reaction.

ACKNOWLEDGEMENTS

The author would like to acknowledge the assistance of those who contributed to this project. He is especially grateful to:

His research director, Dr. T. W. Hoffman, whose enthusiasm and guidance were invaluable.

Cyanamid of Canada Limited, who donated the catalyst.

The National Research Council and the Ontario Research Foundation for their financial assistance.

Dr. R. B. Anderson and Mr. G. R. Stifel who carried out the B.E.T. surface area measurements on the catalyst.

Mr. L. J. Suggett and his staff of the McMaster University Machine Shop who were responsible for the extensive machine shop work involved in this project.

Mr. R. W. Dunn of the Chemical Engineering Department for his assistance in the fabrication and installation of the equipment.

His colleague, Mr. K. G. Pollock, for his many helpful suggestions concerning equipment details.

Miss Jennie M. Sabo for her competent typing of the thesis.

His wife, Olive Lucille, whose encouragement and patience made this work possible.

TABLE OF CONTENTS

LIST OF TABLES

LIST OF FIGURES

NOMENCLATURE

C_{AB}	Concentration of o-xylene in the main gas stream, lb.-moles/ft.^{3} or atm.
C_{AS}	Concentration of o-xylene on the catalyst surface, lb.-moles/ft.^{3} or atm.
C_A	Concentration of o-xylene, lb.-moles/ft.^{3}
C_{Ao}	Inlet concentration of o-xylene, lb.-moles/ft.^{3}
C_{Ps}	Specific heat of catalyst, BTU/lb. °F
C_{PG}	Specific heat of gas, BTU/lb. °F
d_p	Catalyst particle diameter, cm.
D	Molecular diffusion coefficient, cm.^{2}/sec.
ε	Fraction of void space in reactor
F_A	Flowrate of o-xylene, lb.-moles/hr.
F_{Ao}	Feedrate of o-xylene, lb.-moles/hr.
G	Total gas feedrate, lb./hr.
ΔHr	Heat of reaction for complete combustion of o-xylene, BTU/lb.-mole
k	Homogeneous first-order rate constant, sec.$^{-1}$
k_A	Reaction rate constant, ft.^{3}/hr. lb. catalyst
k_G	Mass transfer coefficient, gm.-moles/sec. cm.^{2} atm.
N	Molar flux, gm.-moles/sec. cm.^{2}
N_{SH}	Sherwood number, dimensionless
n	Order of the oxidation reaction

$(-r_A)$	Reaction rate, $\frac{\text{lb.-moles}}{\text{hr. lb. catalyst}}$
ρ_s	True density of catalyst, lb./ft.^{3}
ρ_G	Gas density, lb./ft.^{3}
T	Absolute temperature, °K or °R
t_1	Temperature of solids entering feeder, °F
t_2	Temperature at bottom elbow of reactor, °F
t_3	Temperature at top elbow of reactor, °F
t_4	Temperature of gas sample loop, °F
$\bar{t}$	Average of t_1, t_2, & t_3, °F
V	Reactor volume, ft.^{3}
v_o	Volumetric feedrate of gas to reactor, ft.^{3}/hr.
W_s	Solids feedrate, lb./hr.
X_A	Corrected conversion of o-xylene at reactor outlet
x_A	Conversion due to homogeneous reaction

ABBREVIATIONS

TBR	Transported-Bed Reactor
PA	Phthalic Anhydride
MA	Maleic Anhydride
OTA	O-Tolualdehyde
OX	O-Xylene
OTAc	O-Toluic Acid

1. INTRODUCTION

The method in which the different phases are contacted in heterogeneous chemical reactions has a profound effect on the distribution of reaction products. This is particularly true of catalytic gas-solid reactions such as the oxidation of hydrocarbons. Physical processes of heat and mass transfer are as important as the actual chemical reaction rate in determining the overall rate, or macrokinetics, of the system. The magnitude of the heat and mass transfer resistances depends on the method of contacting the gas and solids. Therefore, the rate of reaction and the yield of desired products can be optimized by proper choice of contacting pattern.

In any chemical reactor, the flow pattern lies somewhere between two ideal extremes: complete mixing, in which the reactant concentration throughout the reactor is that of the effluent stream, and plug flow in which no backmixing is assumed, i.e., each reactant molecule proceeds through the reactor in succession. The presence of two phases complicates the situation because the flow pattern of each phase must be taken into account. In the ideal case, each phase can be in either plug flow or complete backmix flow. For real reactors, a model must be developed which considers the deviations from ideal flow.

The gas-phase catalytic oxidation of hydrocarbons occurs by a complex mechanism which consists of a number of successive (series) and competing (parallel) steps. Invariably the product of industrial interest is one of the intermediate compounds. It has been shown (1, 2)

that the best contacting pattern for reactions in which the desired product is an intermediate is one which minimizes the mixing of fluids of different compositions. Thus, the closer the actual pattern approximates plug flow, the larger the yield of desired product.

A fixed-bed reactor, in which the reactants pass through a stationary bed of catalyst, approaches plug flow conditions. Many hydrocarbon oxidations are effected in a fixed-bed reactor (31, 32). However, a major disadvantage of this type of reactor is the difficulty of achieving isothermal operation. Hydrocarbon oxidation reactions generate a large amount of heat which must be removed quickly in order to maintain isothermal conditions and avoid a runaway reaction. Rapid removal of heat from a packed bed of catalyst is extremely difficult. As a result, hot spots develop in the bed. A temperature rise in the reaction zone of a packed bed of 400°F is not uncommon (3). The effect of hot spots is to lower the yield, reduce the selectivity and increase the hazards of operation. A packed-bed reactor for hydrocarbon oxidations does not lend itself to continuous operation. When it becomes necessary to regenerate the catalyst, either the unit must be shut down or a second bed must be provided so that a reaction-regeneration cycle can be used.

Largely because of hot spots and poor adaptability to continuous operation inherent in a packed-bed reactor, the fluidized-bed reactor has come into widespread use for hydrocarbon oxidation (4). The fluidized bed ensures isothermal operation. Also, catalyst can be continually withdrawn and added, thereby maintaining constant catalytic

activity. Unfortunately, the bubbling, turbulent nature of a fluidized bed which enhances heat transfer is also responsible for its principal deficiency; namely, a wide distribution of residence times. Flow patterns in a fluidized bed are extremely difficult to define (5, 6, 7). Presently, it is thought that the solids approximate backmix flow while the gas flow is closer to backmix than to plug flow. In any case, it is not possible to predict conversion with any degree of certainty. Also, the inability to precisely control the residence time makes it impossible to achieve optimum yields.

The present study is an attempt to carry out the oxidation of a hydrocarbon with a different type of reactor: the transported-bed reactor or dilute fluidized reactor. In this contacting scheme the catalyst, in the form of very small particles, is conveyed upwards by the reacting mixture. Provision is made to continuously re-circulate the catalyst.

The advantages of this method of contacting the gas and solid are:

(a) Both gas and solids approach plug flow. This means that the residence time of both phases is more uniform and can be more precisely controlled. Uniform, precisely-controlled residence time is a prerequisite for yield optimization.

(b) Isothermal operation is easy to achieve. This is due to the relatively large effective heat capacity of the two-phase stream plus the large heat transfer surface of

the solid particles. Even if complete combustion occurs, temperatures will remain at safe levels.

(c) It is easily adaptable to continuous operation. Where deactivation of the catalyst is a problem, fresh catalyst can be added and deactivated catalyst removed continuously. In this way constant catalyst activity can be maintained.

The Transported-Bed Reactor (TBR) has several drawbacks. Principal of these are:

(a) Dilute concentration of catalyst

The voidage in a TBR is always greater than 95%. The relatively small surface area of catalyst per unit volume of reactor restricts this reactor to relatively fast reactions for significant conversion in a reactor of reasonable size.

(b) Catalyst attrition and loss

Continuous circulation subjects the catalyst to buffeting and abrasion. The result is the creation of very fine particles, some of which are lost from the system.

(c) Complicated equipment and operation

In a TBR the catalyst must be continuously removed from the reactor exit stream and fed to the inlet stream. The equipment necessary to accomplish this is complex. Process upsets are difficult to avoid.

2. SYSTEM STUDIED

As the reaction for this study, the gas-phase catalytic oxidation of ortho-xylene over a vanadium pentoxide impregnated catalyst was chosen. This system was selected because of its suitability for a dilute phase reactor and its industrial importance. The oxidation of o-xylene is fast enough (contact times are of the order of a few tenths of a second) to obtain appreciable conversion in a dilute phase reactor. Also, the reaction is highly exothermic, producing up to 10,000 BTU per pound o-xylene feed (8). Consequently, close temperature control is essential.

Industrially, o-xylene competes with napthtalene as the feedstock for the production of phthalic anhydride. The main applications of phthalic anhydride are in plasticizers and surface coatings. Annual U. S. production of phthalic anhydride in 1958 was 350 million pounds (29); this is expected to increase ten-fold by 1975 (4).

3. LITERATURE REVIEW

3.1 Transported-Bed Reactors

Work with transported-bed reactors has been limited because of the requirement that reactions must be extremely fast. However, with the realization that the backmixing characteristics of fluidized beds are detrimental to optimum yields, interest in reactors where residence times can be controlled, such as a transported-bed reactor, has increased. Also, it has been found that much of the gas flowing through a fluidized bed by-passes the bed in bubbles (5) so that the effective gas-solid contact area is reduced. In a transported-bed reactor, on the other hand, all the gas comes in contact with the solids.

Most of the research on transported beds has been carried out by industrial groups so that much of the literature is in the form of patents. An excellent summary of these can be found in the book by Zenz and Othmer (4). A summary of the applications of transported-bed reactors listed in the above reference follows:

(a) Catalytic Cracking of Petroleum Products (38, 44, 45, 46)

A TBR is used before the conventional fluidized reactor-regenerator cracking unit. The products from the TBR are separated in a fractionator, the more volatile products passing out of the system and the heavier products flowing to the conventional cracking unit. A better yield is claimed because not all the gas undergoes the severe cracking conditions of the conventional unit.

(b) Hydrocarbon Synthesis (47)
(Fischer-Tropsch Process)

A feed mixture of carbon monoxide and hydrogen flows concurrently upward with a finely divided metallic catalyst. The TBR is a vertical shell and tube heat exchanger. A high-temperature heat-transfer medium flows through the shell side. This process results in more effective gas-solid contact than in the conventional fluidized bed process, this improvement in gas-solid contact being reflected in higher conversion.

(c) Dilute-Phase Coal Gasification (48)

In the production of water-gas, finely pulverized coal is conveyed upward by a stream of gas and oxygen. The mixture has a residence time of 1.5 to 2 seconds and flows upward at a rate of up to 15 ft./sec.

(d) Dilute-Phase Nuclear Reactor (49)

A dilute-phase nuclear reactor has been developed in which the TBR consists of the moderator material with holes extending through for passage of the fuel-laden gas stream. The fuel is in the form of fissionable dust carried in suspension in an inert gas. Energy produced by the reaction is converted into steam by passing the suspension through a heat exchanger after it leaves the reactor.

(e) Dilute-Phase Acetylene Generator (50)

Russian workers have patented a dilute-phase acetylene generator in which finely ground calcium carbide is conveyed upward by a mixture of recycle acetylene and water.

Klar (9) has patented a transported-bed reactor for the

oxidation of naphthalene or benzene. A spiral member in the reactor imparts a rotation to the upward flowing gas-solid mixture. This action centrifuges the solids to the walls of the reactor such that heat transfer between the reacting mass and the heat transfer medium surrounding the reactor is improved.

In a patent granted to Longwell (40), a reactor for hydrocarbon oxidations is described in which the object is to achieve uniform gas-solid contact time. Reactant gases flow upwards countercurrent to a free-falling stream of catalyst particles descending into the reaction zone. Hence the reaction occurs in the dilute phase. Catalyst collecting at the bottom of the reactor is recirculated by a pneumatic conveying line. Yields of phthalic anhydride of 87% with complete conversion from the oxidation of naphthalene are reported.

3.2 Mechanism and Kinetics of the Vapour Phase Catalytic Oxidation of O-Xylene

Because of the complexity of the reaction and the difficulty in accurately analyzing the product mixture, the mechanism is poorly understood. Confusion exists as to the sequence of steps in the reaction, the adsorption of components on the catalysts, and rate-controlling steps in the process.

Simard et al. (21) studied the reaction in a fixed-bed reactor at 400 to 450°C, contact times of .01 to .06 second, and o-xylene concentrations in air of 0.4 to 1.4%. The catalyst was V_2O_5 supported on silicon carbide. They proposed the following mechanism:

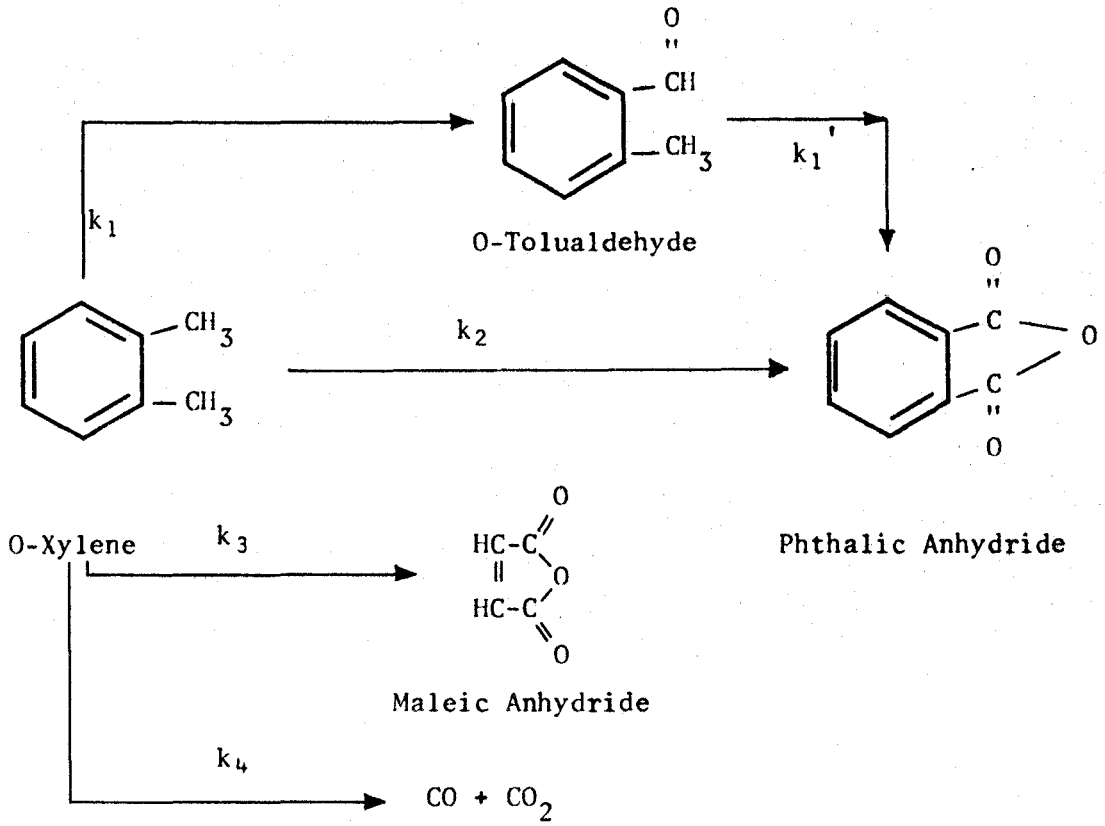

Reactions 1 and 1' were found to be first order with respect to o-xylene and o-tolualdehyde while the remaining reactions were all zero-order in o-xylene. The authors concluded that the individual oxidation reactions take place on the catalyst surface and that the oxygen comes from the catalyst itself. Re-oxidation of the catalyst by oxygen from the gas stream was thought to be the rate-controlling step. A square root dependence on oxygen pressure of all reactions was taken as evidence of this.

In a more recent investigation, Novella and Benlloch (16, 17, 18) studied the reaction in a fluidized bed (see Table 1 for reaction conditions). Based on the observed product distribution, these workers deduced a seven-step mechanism:

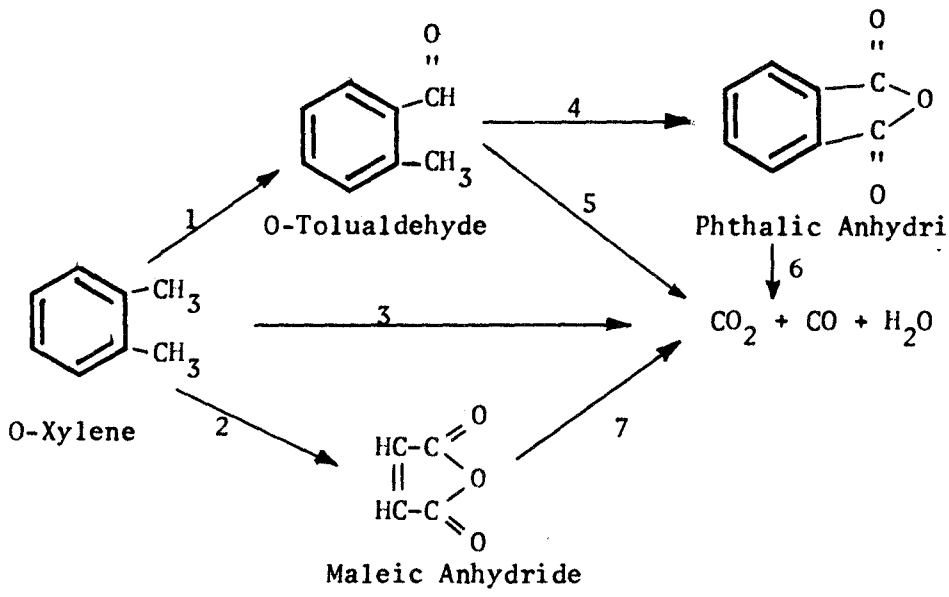

10

All the reactions were found to be elementary, i.e., first-order. All occurred by the same mechanism: reaction on the catalyst surface between the hydrocarbon from the gas phase and the chemisorbed oxygen of the catalyst, the surface reaction rate being rate-controlling. With the large excess of oxygen in their study, the resistance to chemisorption of oxygen was stated to be negligible.

Simard et al. (19) studied the composition of V_2O_5 catalysts during the course of oxidation of o-xylene. After a reaction period, the catalyst (originally containing only V_2O_5) contained a mixture of V_2O_5, V_2O_4, and $V_2O_{4.34}$. Upon overloading the feed with o-xylene (3.3 mole %), catalytic oxidation stopped completely and the catalyst was completely reduced to V_2O_4 and V_2O_3. These observations, plus the fact that a high yield of phthalic anhydride was obtained with a feed of o-xylene in nitrogen, tend to confirm that the oxidation occurs between the hydrocarbon from the gas phase and oxygen of the catalyst.

Vrbaski and Mathews approached the problem by studying the oxidation of o-methylbenzyl alcohol (35) and o-tolualdehyde (36), in a fixed-bed of fused V_2O_5. Both these compounds have been isolated as

intermediates in hydrocarbon oxidations and a knowledge of their oxidation mechanism should help clarify the mechanism of o-xylene oxidation. In the o-methylbenzyl alcohol study, the isolatable products were o-tolualdehyde, per-o-toluic acid, o-toluic acid, o-xylene, phthalide, phthalic anhydride, maleic anhydride, carbon monoxide, and carbon dioxide. Below 390°, o-tolualdehyde was the principal product. Above 380°, phthalic anhydride began to form. At about 425°C, phthalic anhydride was the principal product. The data were represented by the reaction scheme:

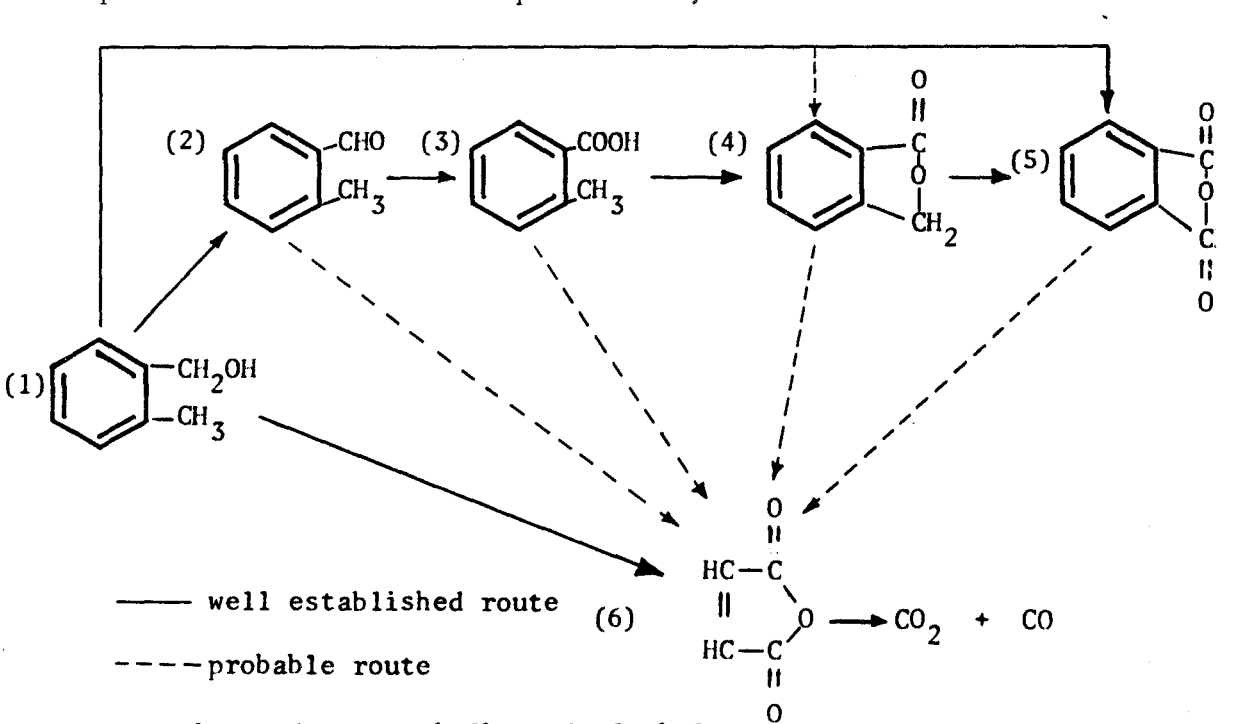

where 1 = o-methylbenzyl alcohol

2 = o-tolualdehyde

3 = o-toluic acid

4 = phthalide

5 = phthalic anhydride

6 = maleic anhydride

A similar mechanism was deduced for the oxidation of o-tolualdehyde (36). Below 390°C o-toluic acid was the main product. Above 390°C the formation of phthalic anhydride increased rapidly and passed through a maximum at about 430°C. O-tolualdehyde was oxidized to phthalic anhydride by either a step-wise route (via o-toluic acid and phthalide) or by a direct route. Lower temperatures favoured the sequential oxidation while at higher temperatures the direct oxidation step predominated. Steady-state conditions as defined by Hinshelwood exist on the catalyst surface. This means that the rate of adsorption of oxygen and the rate of adsorption of o-tolualdehyde are of the same order of magnitude as the surface reaction rate.

Mann (37) also applied the steady-state concept. He investigated the kinetics and mechanism of o-xylene oxidation over a V_2O_5 - K_2SO_4 silica catalyst at 300 - 334°C. The data were found to fit the steady-state adsorption model with some reservations. This model assumes that a steady-state concentration of adsorbed oxygen exists on the catalyst surface. Therefore, the rate of adsorption of oxygen must equal the rate of reaction between adsorbed oxygen and hydrocarbon in the gas. An alternative to the steady-state model is the Langmuir-Hinshelwood model. Here it is assumed that an equilibrium exists between oxygen in the gas phase and oxygen adsorbed on the catalyst surface. For this to be true the rate of adsorption of oxygen must be much larger than the rate of surface reaction. Mann concludes that the oxygen adsorption rate is relatively slow and equilibrium cannot be assumed. The main products

from Mann's work were o-tolualdehyde, phthalic anhydride, carbon dioxide and carbon monoxide. No maleic anhydride was reported.

Satterfield and Loftus made an interesting study (24, 27) in which a mixture of nitrogen and o-xylene was bubbled through a V_2O_5 - K_2SO_4 eutectic melt at 528 - 598°C. They obtained a product distribution similar to that from the solid catalyzed reaction except no phthalic anhydride or maleic anhydride was produced. It was concluded that the liquid-gas interface was as reactive as the solid-gas interface but was incapable of producing phthalic anhydride. This work emphasizes the importance of the physical characteristics of the catalyst in determining the product distribution.

3.3 Yield-Optimization Studies

Most of the o-xylene oxidation studies have been empirical and have concentrated on optimizing the yield of phthalic anhydride. The important variables are reaction temperature, contact time, air to o-xylene ratio in the feed, type of catalyst, and type of reactor (fluidized or fixed bed). Table 1 summarizes the optimum conditions and corresponding yields.

Several conclusions can be drawn from the optimization work:

(a) The nature of the catalyst influences the product distribution. The wide variation in optimum conditions found by different workers can probably be attributed to differences in catalysts used.

(b) The maximum yield of phthalic anhydride is 72% of theoretical

TABLE 1

OPTIMUM CONDITIONS AND PRODUCT YIELDS FOR CATALYTIC OXIDATION OF O-XYLENE

COMPARISON OF RESULTS OF VARIOUS WORKERS

REF.	REACTOR	TEMP., °C.	PRODUCT YIELD, % (iv)				SPACE TIME (v)	AIR/XYLENE	CATALYST
			PA	MA	OTA	OTHER (iii)	SEC.	MOLE/MOLE	
10	Fixed Bed	440	42.7	11.3	--	24.5	0.625	340	V_2O_5 on Kr (i) (31.1 : 100)
11, 12	Fixed Bed	490	61.7	9.6	--	18.5	0.625	274	Fused V_2O_5 (ii) (unsupported)
13, 14, 15	Fluidized Bed	490	67.8	--	3.6	16.6	0.358	95	Fused V_2O_5
16	Fluidized Bed	310	52.0	15.0	2	2.7	14	334	V_2O_5 : K_2SO_4 : Silica Gel (10 : 33 : 57)
20	Fixed Bed	550	40.8	5.1	2.5	18	0.12	103	Fused V_2O_5 on granular Aluminum carrier
22	Fixed Bed	530	15.3	--	Tr	0.5	0.18	126 (vi)	V_2O_5 supported on Alfrax
23	Fluidized Bed	460	18	5	Tr	1	1.9	185	V_2O_5 supported on Silica 31.2 : 100
3	Fixed Bed (vii)	610	98	--	--	--	0.02	73	V_2O_5 supported on Silicon Carbide 15 : 85
28	Fixed Bed	427	60	Tr	--	Tr	N.A.	24	V_2O_5
29, 30, 31	Fixed Bed (viii)	380	65	N.A.	N.A.	N.A.	0.1 - 0.2	72	V_2O_5 : K_2SO_4 : Silica Gel 10 : 25 : 65
29, 30, 31	Fluidized Bed (viii)	460	72	N.A.	N.A.	N.A.	0.5 - 1.0	46	V_2O_5 : K_2SO_4 : Silica Gel 10 : 25 : 65
41	Fluidized Bed	450	67	7	N.A.	N.A.	2.4	100	Fused V_2O_5 on Silica Gel 25 : 75

Tr = Trace N.A. = Information not available

FOOTNOTES - TABLE 1

(i) Unfused V_2O_5 on Indian Kieselguhr

(ii) Fused V_2O_5 prepared by heating ammonium metavanadate to fusion point, cooling, breaking up, and screening to desired size

(iii) Mainly CO_2

(iv) Calculated as $\frac{\text{Moles Product Formed}}{\text{Moles O-X Fed}} \times 100\%$

(v) S.T. = $\frac{\text{Vol. of catalyst bed (voids + solids), cc.}}{\text{Vol. feedrate of gas mixture @ STP cc./sec.}}$

(vi) Feed a mixture of xylenes; ortho- & meta- predominating

(vii) Reactor equipped with a device for rapidly cooling the products to 260°C immediately following the catalyst bed

(viii) Summary of industrial practice

and is attained in a fluidized-bed reactor.

(c) Most workers conclude that a fluidized bed is superior to a fixed bed, claiming:

(i) better control of reaction conditions.

(ii) higher yield of desired products.

(iii) absence of explosion hazard.

(iv) greater throughput per unit volume of catalyst.

3.4 Homogeneous Reaction

Knowledge of the rate of homogeneous oxidation of o-xylene, i.e., with no catalyst, is important because it gives an indication of how much of the observed reaction is catalytic. Also, it has been shown (33, 34, 25, 26) that the homogeneous reaction does not form phthalic anhydride so that the overall yield will be reduced by homogeneous oxidation.

Wright investigated the homogeneous oxidation (33, 34) at 650°C and isolated 38 oxidation products. Carbon dioxide, carbon monoxide, methane, hydrogen, water, and toluene were the major products.

Satterfield and Loftus (25, 26) determined the rate of homogeneous oxidation at lower temperatures (450 - 550°C). The major products were o-xylene oxide, o-tolualdehyde, and benzene. The rate of reaction was first-order with respect to o-xylene. The rate constant was given by

$$\ln k = 10.05 - 20{,}000/RT$$

where k is the first order rate constant in sec^{-1} and the activation energy is 20,000 cals/gm. mole.

4. SCOPE OF THIS WORK

This thesis is an exploratory study to investigate the feasibility of conducting the catalytic, vapour-phase oxidation of o-xylene in a transported-bed reactor.

The primary purpose of this work was to study the effects of a unique contacting pattern on the distribution of reaction products. Obtaining kinetic data about the reaction was a secondary objective.

The reaction was investigated at a contact time of 0.2 seconds, air-to-o-xylene molar ratios of 42 to 86, solids-to-gas weight ratios of 8 to 23, and a reaction temperature of approximately 750°F (400°C).

Reaction products were analyzed by Gas-Liquid Chromatography and Nuclear Magnetic Resonance Spectroscopy. The analytic method could not detect carbon dioxide, carbon monoxide, or water in the product stream.

5. EXPERIMENTAL DETAILS

5.1 Reactor and Associated Equipment

This section is divided into two parts. In the first, a general description of the flow system is given. Following this, the individual units of the system are discussed in detail. In addition to the information given in this section, Appendix 4 lists complete equipment specifications.

5.1.1 Description of Flow

Figure 1 is a flow diagram of the apparatus. Numbers in brackets in the text correspond to the numbers on this diagram.

The source of air is a 100 psi main (1). After passing through two filters in series (2), the air enters the flow control system, consisting of an orifice plate (3), a transmitter (4), a controller (5), and a control valve (6). The flow-control system is a conventional orifice-meter type and operates with proportional plus reset mode. A rotameter (7) indicates the magnitude of the air flow.

From the rotameter, air flows into the air heater (8). This heater is a shell and tube exchanger with 100 psi steam on the shell side. Air leaving the heater (at a temperature of approximately 300°F) flows into the carburetor (9) where the o-xylene stream is vaporized and the air-o-xylene mixture is heated. O-xylene is fed to the carburetor from a feed tank (10) which is pressurized with nitrogen. O-xylene flow is controlled with a diaphragm valve (11) and indicated by a rotameter (12). The carburetor, a vessel packed with 1/4 in. Raschig rings and jacketted

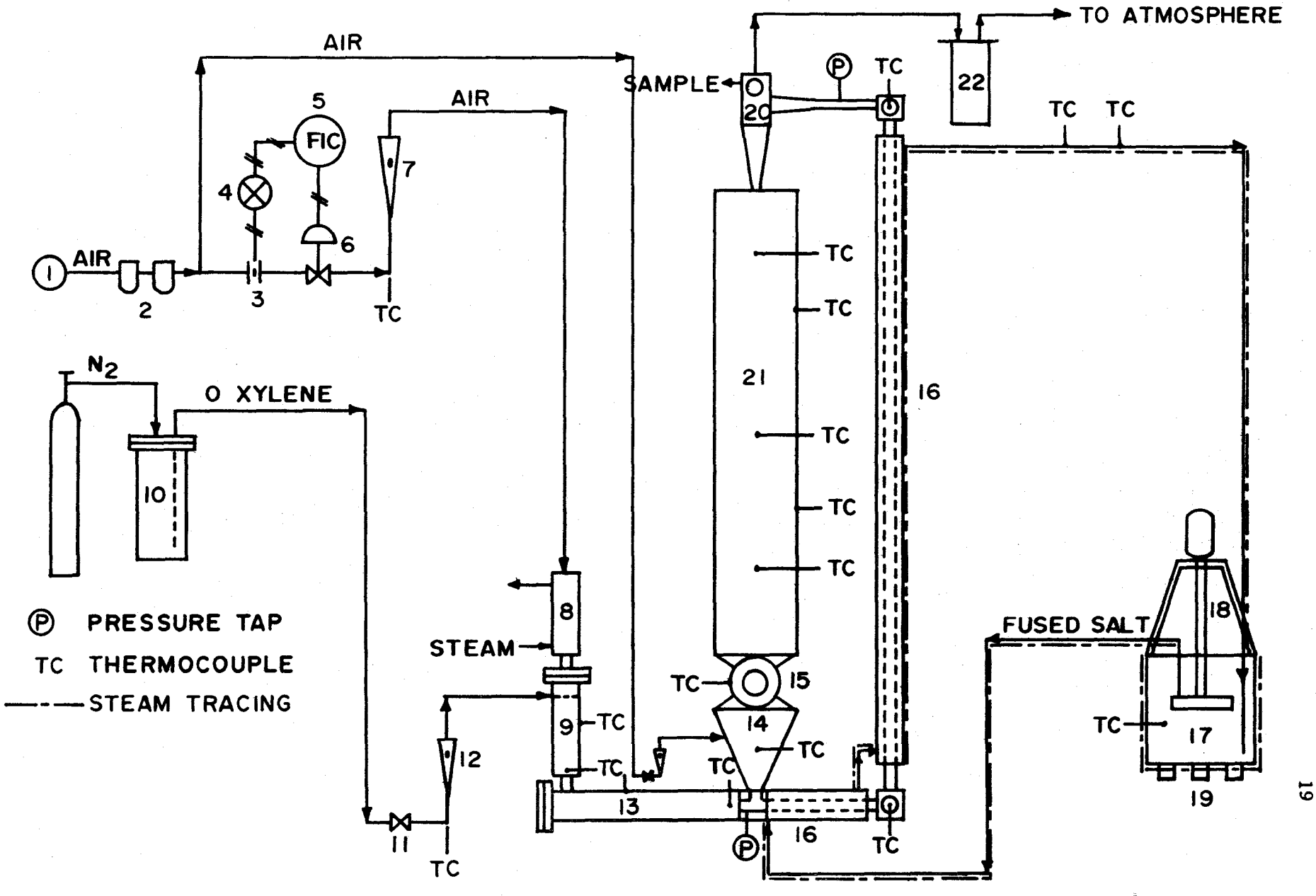
AIR
AIR
AIR
5
FIC
4
6
7
1
2
3
TC
N2
O XYLENE
10
P PRESSURE TAP
TC THERMOCOUPLE
STEAM TRACING
8
STEAM
9
TC
TC
12
11
TC
13
SAMPLE
20
P
TC
22
TO ATMOSPHERE
TC
TC
21
TC
TC
TC
TC
16
TC
15
14
TC
TC
TC
16
P
TC
FUSED SALT
18
TC
17
19
19

with electrical heaters, heats the air-hydrocarbon mixture to approximately 600°F.

The reactant mixture is then heated to the reaction temperature in the preheater (13) which is also electrically heated. Immediately downstream from the preheater is the zone in which the gas comes in contact with the catalyst. Here the solid particles become suspended in the gas stream.

Catalyst is metered into the gas stream with a rotary solids feeder (15) which discharges the solids into a discharge cone (14) and then into the suspension zone. A variable-speed drive, connected to the rotor of the solids feeder with a slip clutch, controls the feedrate of catalyst.

The gas-solid mixture flows cocurrently up the reactor (16). At the top of the reactor, the solids are separated from the reacting gases by a cyclone separator (20). Solids drop from the separator, through a section of flexible bellows, and into the solids hold-up tank (21).

A fused salt system, consisting of a tank (17) and a pump (18), controls the reaction temperature. Molten salt circulates through an annulus formed by the reactor and a jacket. The salt temperature and hence the reaction temperature is controlled by electrical immersion heaters (19) in the salt tank.

The gas stream leaving the top of the cyclone flows into a water-cooled trap (22). The effluent from the trap is exhausted to atmosphere. A sample stream is withdrawn from the main stream at the

top of the cyclone.

A small amount of air flows from a tee in the air supply line, through a needle valve and rotameter, and into the solids discharge cone. This air flow, termed auxiliary air, is required to prevent the solids from "bridging" in the discharge cone. Initially an electrical vibration unit was mounted to the solids discharge cone in order to maintain steady solids flow. However, this unit did not noticeably affect solids feeding so it was removed.

Temperatures can be measured at 18 different points in the system with thermocouples, indicated by T.C. on the flow diagram. Recorder terminals are mounted on a control panel so that all temperatures can be continuously monitered from one location.

5.1.2 Description of Individual Units

(a) Air Flow Control System (Figure 2)

Air for reactor feed, coming from the filters, flows through a 24 in. straight section of 0.68 in. I.D. stainless steel tubing, the orifice plate, a 12 in. straight section of 0.68 in. I.D. stainless steel tubing, the control valve, and finally to the rotameter via 1/2 in. copper tubing.

The flow of air through the orifice plate causes a pressure drop. This differential pressure is transmitted to the transmitter with 1/4 in. copper tubing. A 1/2 in. Whitey Vee Stem regulating valve is located in each pressure transmitting line. A by-pass line is provided between the high and low pressure leads so that the pressure can be

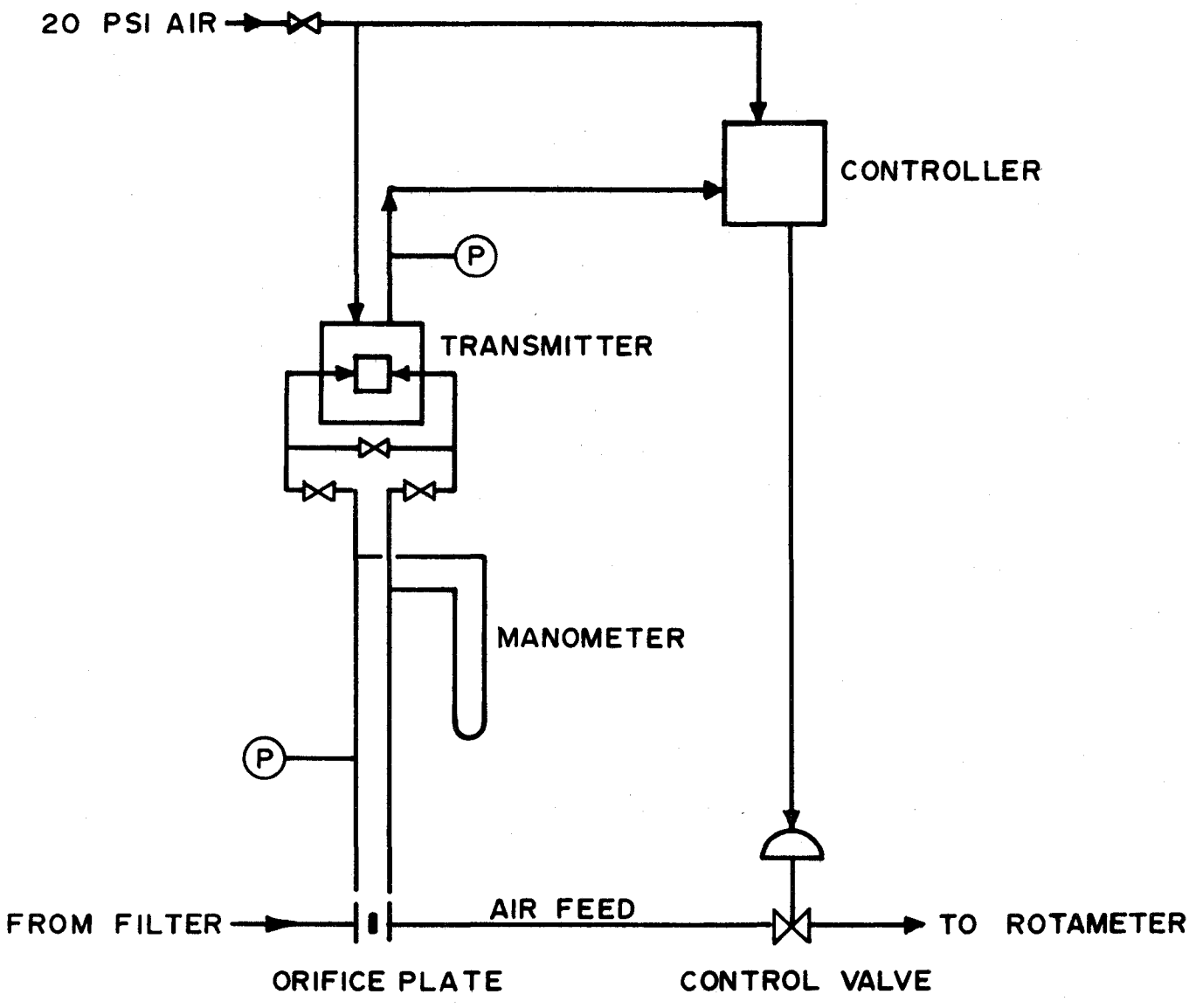
20 PSI AIR
CONTROLLER
P
TRANSMITTER
MANOMETER
P
FROM FILTER
AIR FEED
TO ROTAMETER
ORIFICE PLATE
CONTROL VALVE

equalized when desired. The by-pass line is opened or closed with a 1/4 in. Whitey toggle valve.

The transmitter, a Minneapolis Honeywell Differential Converter, maintains a pneumatic balance between the differential pressure, the transmitted pressure, and the 20 psi supply pressure. This results in a pressure directly proportional to the differential pressure across the orifice being transmitted to the controller. The line from the transmitter to the controller is 3/8 in. copper tubing as is the 20 psi air line to the transmitter and to the controller.

The controller is a United States Gauge Indicating Pilot Controller with proportional plus reset action. Depending on whether the pressure from the transmitter is lower or higher than the set point pressure, the controller output pressure either opens or closes the diaphragm control valve. The line from the controller to the control valve is 3/8 in. copper tubing.

A panel-mounted manometer indicates the differential pressure across the orifice. The legs of the manometer are 3/8 in. O.D. x .094 wall Pyrex glass, and the "U" is formed by two 3/8 in. stainless steel Swagelok elbows joined by a 1 1/2 in. length of 3/8 in. O.D. x .035 in. wall stainless steel tube. The glass legs are sealed in the elbows with Teflon sleeves. Connections from the copper lines to the manometer are with brass Swagelok fittings and Teflon sleeves.

(b) Carburetion System (Figure 3)

The carburetor was constructed from a 1 ft. section of

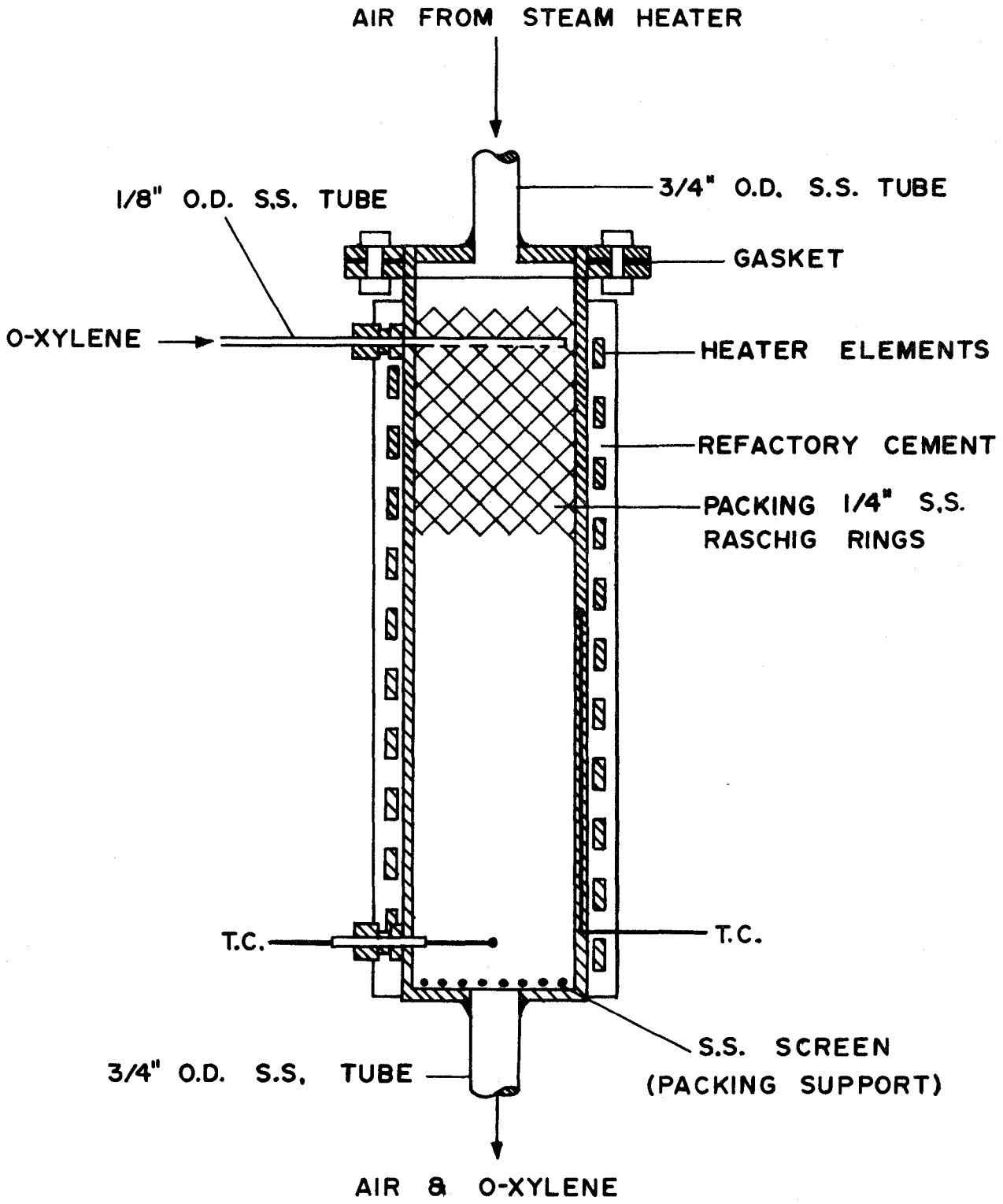
AIR FROM STEAM HEATER
1/8" O.D. S.S. TUBE
3/4" O.D. S.S. TUBE
GASKET
O-XYLENE
HEATER ELEMENTS
REFACTORY CEMENT
PACKING 1/4" S.S.
RASCHIG RINGS
T.C.
T.C.
S.S. SCREEN
(PACKING SUPPORT)
3/4" O.D. S.S. TUBE
AIR & O-XYLENE

316 stainless steel 2 1/2 in. nominal diameter schedule 40 pipe. The ends were cut from 1/4 in. stainless steel plate. The bottom end is welded to the pipe and the top is removable, being joined to the pipe by a flange connection. This connection is sealed with a Klinger 1000 gasket.

Air from the steam heater enters the top of the carburetor through a section of 3/4 in. O.D. x .035 in. wall stainless steel tube. O-xylene enters the carburetor just below the flange through a section of 1/8 in. O.D. x 0.049 in. wall stainless steel tube. O-xylene flows into the carburetor from 1/16 in. diam. holes drilled in the underside of the inlet tube. This distributes the flow across the diameter of the carburetor. The o-xylene inlet tube is fixed in place with a 1/8 in. stainless steel Swagelok cap which is welded to the carburetor wall and drilled through. The air-o-xylene mixture discharges from the carburetor through a section of 3/4 in. O.D. x .035 in. wall stainless steel tube.

The carburetor is packed with 1/4 stainless steel Raschig rings to insure a large gas-liquid contact surface. The packing is supported by a heavy stainless steel screen which rests on the bottom plate of the carburetor.

Temperatures are measured by two chromel-alumel thermocouples. One measures the temperature of the gas mixture leaving the carburetor and the other measures the wall temperature at the midpoint. Both thermocouples are made from 1/16 in. O.D. Ceramo thermocouple wire. The wall thermocouple was positioned by drilling a hole in the wall,

placing the hot junction tip into this hole, and peening the edge of the hole over the tip. The interior thermocouple enters the carburetor through a 1/8 in. stainless steel Swagelok cap which is welded to the carburetor wall and drilled through. A 1/8 in. stainless steel sleeve is silver-soldered to the thermocouple sheath where it passes through the fitting. Unless stated otherwise, all thermocouples mentioned in subsequent descriptions are installed in this fashion. This method of installing the thermocouple was adopted to allow the removal and replacement of the thermocouple if necessary. In practice, it was found that extreme heat tended to weld the thermocouple to the fitting so that removal was impossible.

Heat input to the carburetor is by electrical heaters. The heating element is Kanthal A-1 resistance strip wound spirally around the carburetor. Heat input is 1500 watts at 24 volts. Electrical insulation is with Hiloset refractory cement. The heaters were operated with a low voltage and high current to avoid the possibility that the insulating cement becomes conducting at high temperatures. The power supply is 230 volts. This is transformed with a 10:1 step down transformer. Complete details of the transformer circuitry can be found in the thesis by Dernedde (51). Power output from the transformer is controlled by a powerstat.

The entire carburetor is insulated with 2 1/2 in. nominal diameter x 2 in. thick Johns-Manville Thermobestos insulation.

(c) Reactant Preheating and Solids Suspension System (Figure 4)

The reactant preheater was constructed from a 2 ft. section of 316 stainless steel 2 1/2 in. nominal diameter schedule 40 pipe. The heating assembly consists of two units, each identical to the carburetor heaters. With this arrangement, heat input to each half of the preheater can be independently controlled.

Baffles are spaced at 1 in. intervals inside the preheater. These baffles are 1/16 in. stainless steel and are cut so that 80% of the cross section of the preheater is covered. They are mounted with the cut edge alternately up and down.

The location of thermocouples in the preheater is similar to the carburetor, one thermocouple measuring the wall temperature at the midpoint and the other measuring the gas discharge temperature. The mounting procedure is identical to that described for the carburetor. The wall thermocouple is made from 1/16 in. chromel-alumel Ceramo while the interior thermocuple is 1/16 in. platinum-platinum 10% rhodium Ceramo. Platinum-platinum 10% rhodium thermocouples were employed rather than chromel-alumel wherever there was a possibility of the hot junction being oxidized.

Catalyst is fed into the gas stream immediately downstream from the preheater. The catalyst-gas mixing zone and the first section of the reactor are an integral unit. The catalyst gas mixing zone is machined from 316 stainless steel bar stock, the reactor is 3/4 in. O.D. x .035 in. wall stainless steel tubing, and the reactor jacket is 1 1/8 in. O.D. x .035 in. wall stainless steel tubing.

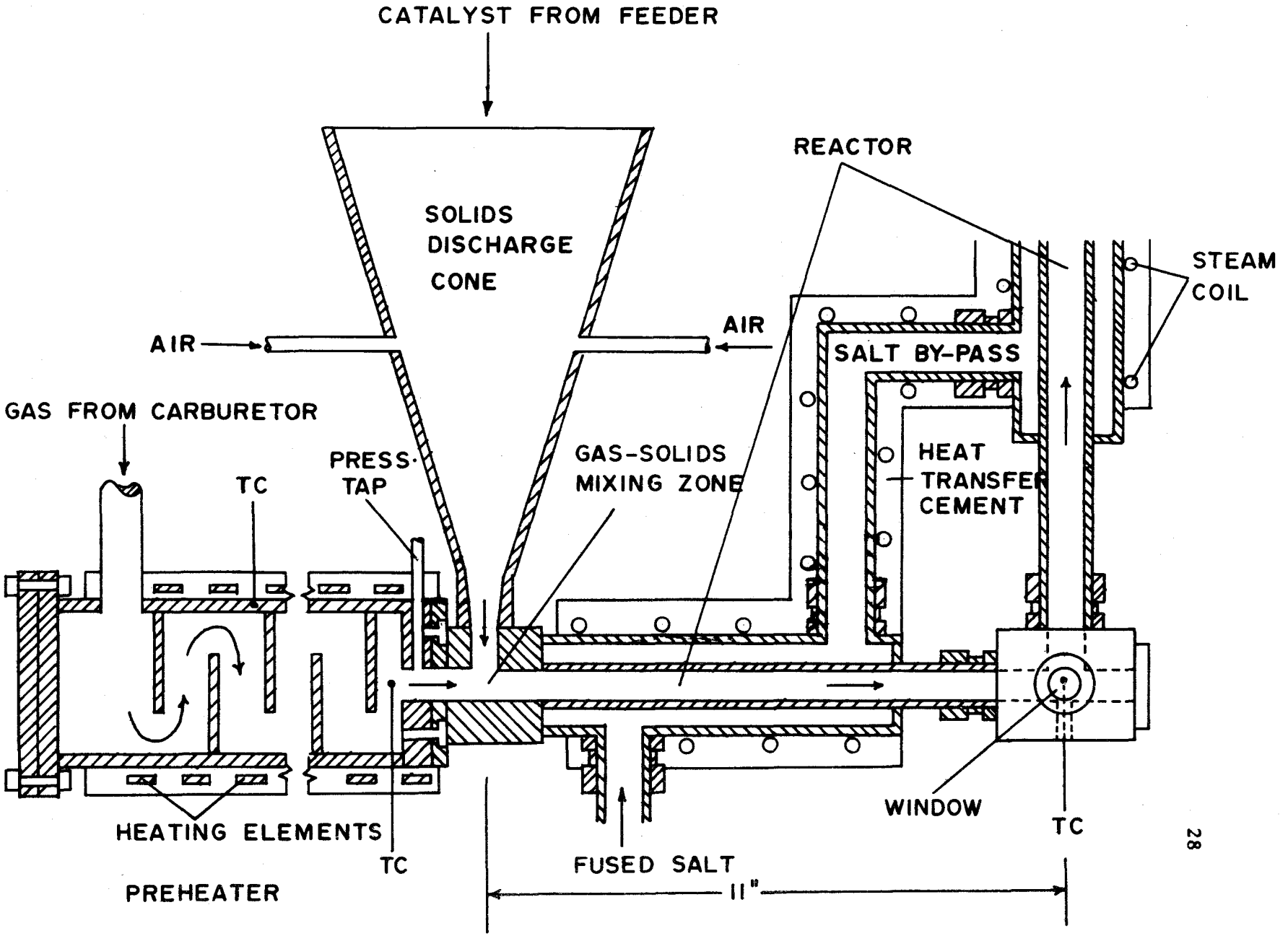
CATALYST FROM FEEDER
REACTOR
SOLIDS
DISCHARGE
CONE
STEAM
COIL
AIR
AIR
SALT BY-PASS
GAS FROM CARBURETOR
PRESS.
TAP
TC
GAS-SOLIDS
MIXING ZONE
HEAT
TRANSFER
CEMENT
HEATING ELEMENTS
TC
WINDOW
TC
PREHEATER
FUSED SALT
11"

The solids discharge cone is bolted with a flange connection to the gas-solid mixing zone. The solids discharge cone was rolled from 1/16 stainless steel. Two auxiliary air jets are located at diametrically opposite points at the midpoint of the discharge cone. Also located at this level is a chromel-alumel thermocouple. Auxiliary air flows into the cone via 1/4 in. O.D. x .035 in. wall stainless steel tubing.

The gas-solids mixture flows horizontally up to an elbow where it makes a 90 degree bend. The elbow, machined from stainless steel bar stock, contains two observation windows, a removable cover (for cleaning purposes), and a Platinum-Platinum 10% Rhodium thermocouple. The observation windows, made of Vycor glass, fit into 3/4 in. holes drilled on opposite sides of the elbow. A 3/4 in. ring of Klinger 1000 gasket material is first fitted into the hole, then the glass, then another gasket ring and finally a stainless steel ring which is bolted to the elbow to hold the assembly in place.

Fused salt from the circulation pump enters the reactor jacket immediately downstream of the gas-solids mixing zone. Entry is through a 3/4 in. stainless steel Swagelok cap which is welded to the outside of the jacket and drilled through. The salt solution by-passes the observation elbow through a 90° bend made of two sections of 3/4 in. O.D. x .035 in. wall stainless steel tubing welded at right angles. The fittings at the entrance and exit of this bend are identical to the salt inlet fitting.

The reactor is stream-traced with 3/8 in. copper tubing wound spirally around the reactor jacket and salt by-pass. The steam supply is at 335°F and 100 p.s.i.g. Thermon high-temperature heat-transfer cement was applied to the spaces between the copper coil and the surface to improve heat transfer.

The preheater, gas-solids mixing zone, solids discharge cone, reactor, and elbow are insulated with 2 in. thick Johns-Mannville Thermobestos pipe insulation. Irregular shapes are insulated with asbestos insulating cement.

A pressure tap is located at the outlet of the preheater before the solids and gas streams meet. This tap was constructed by drilling a 1/8 in. hole in the end plate of the preheater perpendicular to the longitudinal axis. A 3 in. section of 1/8 in. stainless steel tubing is welded to the end plate so that the centerline of the tubing and the centerline of the hole are concurrent. A filter is located at the end of the section of tubing. The filter is a Gelman Instrument 1 in. stainless steel filter holder with a Type A glass fiber filter. From the filter the pressure is transmitted to a gauge on the control panel with 1/4 in. copper tubing.

(d) Gas-Solid Separation (Figure 5)

The cyclone design is based on the high efficiency cyclone described by Stairmand (52). It is designed to have a gas inlet velocity of 50 ft./sec. With this inlet velocity, Stairmand reports a collection efficiency -- defined as the percentage of solids collected of a particular

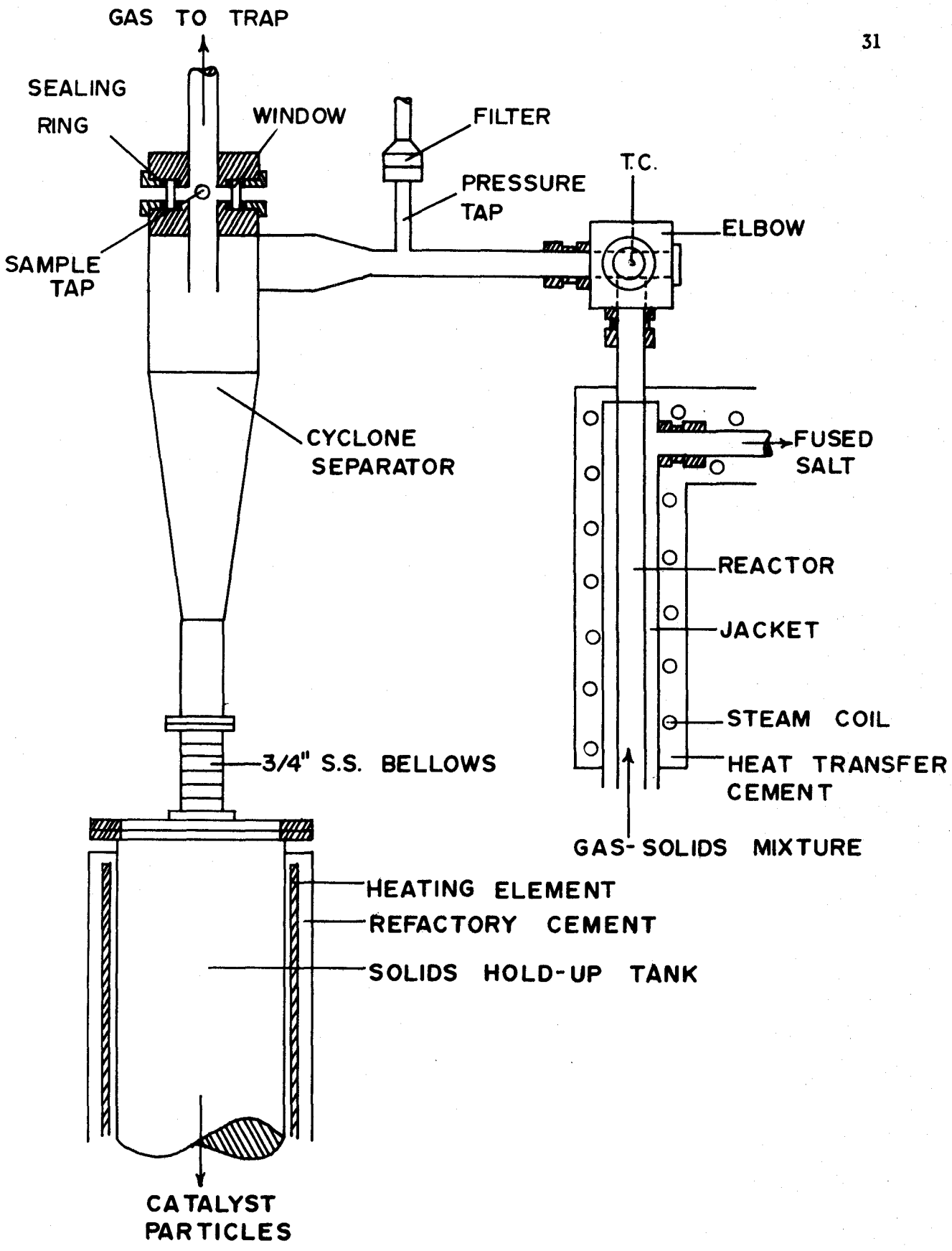
GAS TO TRAP
SEALING RING
WINDOW
FILTER
T.C.
PRESSURE TAP
ELBOW
SAMPLE TAP
CYCLONE SEPARATOR
FUSED SALT
REACTOR
JACKET
STEAM COIL
3/4" S.S. BELLOWS
HEAT TRANSFER CEMENT
GAS-SOLIDS MIXTURE
HEATING ELEMENT
REFACTORY CEMENT
SOLIDS HOLD-UP TANK
CATALYST PARTICLES

size relative to the amount of that size in the feed -- of 85% for 5 micron particles of density 2 gm./c.c. Included in the above reference are transformation factors to apply to the collection efficiency to account for different operating conditions. Applying these factors to the conditions of this study, the collection efficiency for 5 micron particles is 70%.

At the top of the vertical section of the reactor, the gas-solids mixture enters an elbow identical to the bottom elbow described in the preceding section. The vertical distance from centerline to centerline of the elbows is 12 ft. 7 in. From the top elbow, the reacting mixture flows through a horizontal section of 3/4 in. O.D. x .035 in. wall stainless steel tubing. At the discharge of this section is a swaged section that changes the cross-section from circular to 1.67 in. x 0.67 in. rectangular. The catalyst-laden gas enters the cyclone through this rectangular section which is welded so that the inlet to the cyclone is tangential.

As the mixture rotates in the cyclone, the solids migrate to the wall, under the influence of centrifugal forces, and discharge through the bottom of the cyclone to the solids hold-up tank. The essentially catalyst-free gas flows from the top of the cyclone through a central vortex which extends the length of the unit.

At the top of the cyclone, provision is made to sample the gas stream and to observe the condition of this stream. The material and installation of the observation windows is identical to that of

the elbows. The sample outlet is a section of 1/8 in. O.D. stainless steel tubing. A 1 in. stainless steel Gelman filter holder with a Type A glass fiber filter is located in the sample line to prevent any catalyst particles from entering the analysis system. From the filter, the sample flows through an electrically-heated section of 1/8 in. O.D. stainless steel tubing to the analytical apparatus.

From the top of the cyclone, the gases flow via 1 in. steel pipe to the water-cooled trap. This is a 24 in. section of 4 in. I.D. Pyrex glass pipe with flange-connected brass end plates. Gases enter and leave the trap at the top. Cooling is provided by circulating tap water through a 50 ft. section of 1/4 in. copper tubing coiled inside the trap. Gases leaving the trap are exhausted through 1 in. steel pipe to a fan and thence to atmosphere.

The support of the reactor and solids hold-up tank is such that the unit can expand freely in the vertical direction as the temperature increases. An 18 in. section of 3/4 in. stainless steel bellows is silver-soldered in the line from the top of the cyclone to the cold trap. This allows for differential expansion.

Solids drop from the bottom of the cyclone into the solids hold-up tank. The cyclone is connected to the hold-up tank with a 3 in. long section of 1 1/8 in. diameter stainless steel bellows which is flange-connected at each end. These bellows relieve any stresses caused by thermal expansion.

The solids hold-up tank is 9 ft. in length x 6 in. in diameter

and was rolled from 1/16 in. stainless steel sheet. It is connected to the cyclone at the top and to the solids feeder at the bottom by flange-connections. The walls of the hold-up tank are electrically heated, the heating element consisting of six strips of Kanthal A-1 heating strip mounted on the outside of the tank parallel to the longitudinal axis. Each pair of heating elements is connected in parallel to a variable 24 volt power source, giving three independently variable heaters, each with a maximum power input of 1700 watts. Electrical insulation of the heating elements is with Hiloset cement. Temperatures are measured at five locations in the hold-up tank with 1/16 in. Chromel-Alumel Ceramo thermocouples. Wall temperatures are measured at the 3 and 6 ft. levels and interior temperatures at the 1 1/2, 4 1/2, and 7 1/2 ft. levels. Details of thermocouple installation are identical to those described earlier (section 5.1.2 (b)).

A pressure tap is located in the gas-solids inlet line to the cyclone immediately upstream of the swaged section. The tap was made by welding a 3 in. length of 1/8 in. O.D. stainless steel tubing to the line and drilling through. At the end of this 3 in. section is a Gelman filter identical to that used for the sample line. From the filter, a 1/4 in. copper tube line transmits the pressure to a gauge on the control panel.

The equipment described in this section is insulated with two inches of Thermobestos pipe insulation.

(e) Catalyst Feeding System (Figure 6)

The solids feeder, flange-connected to the bottom of the solids hold-up tank, is a rotary valve. Each revolution of the rotor transfers a fixed volume of catalyst from the hold-up tank to the solids discharge cone. The clearance between the edges of the rotor and the valve housing is small (ca. 0.005 in. at room temperature) in order to prevent reacting gases from blowing up through the valve.

In practice, however, the ability of the valve to prevent the upward flow of gas was poor. A certain amount of gas did by-pass the reactor and flow through the valve. As the gas flow through the valve increased, the solids feedrate dropped markedly. The amount of gas by-passing the reactor depended on the height of the catalyst bed above the valve, contrary to what would be expected if the valve acted as an air seal.

The solids feeder has the following components:

(i) rotor and shaft
(ii) housing
(iii) end plates
(iv) external bearing
(v) coupling
(vi) variable speed drive
(vii) heaters

Each component will be discussed in turn.

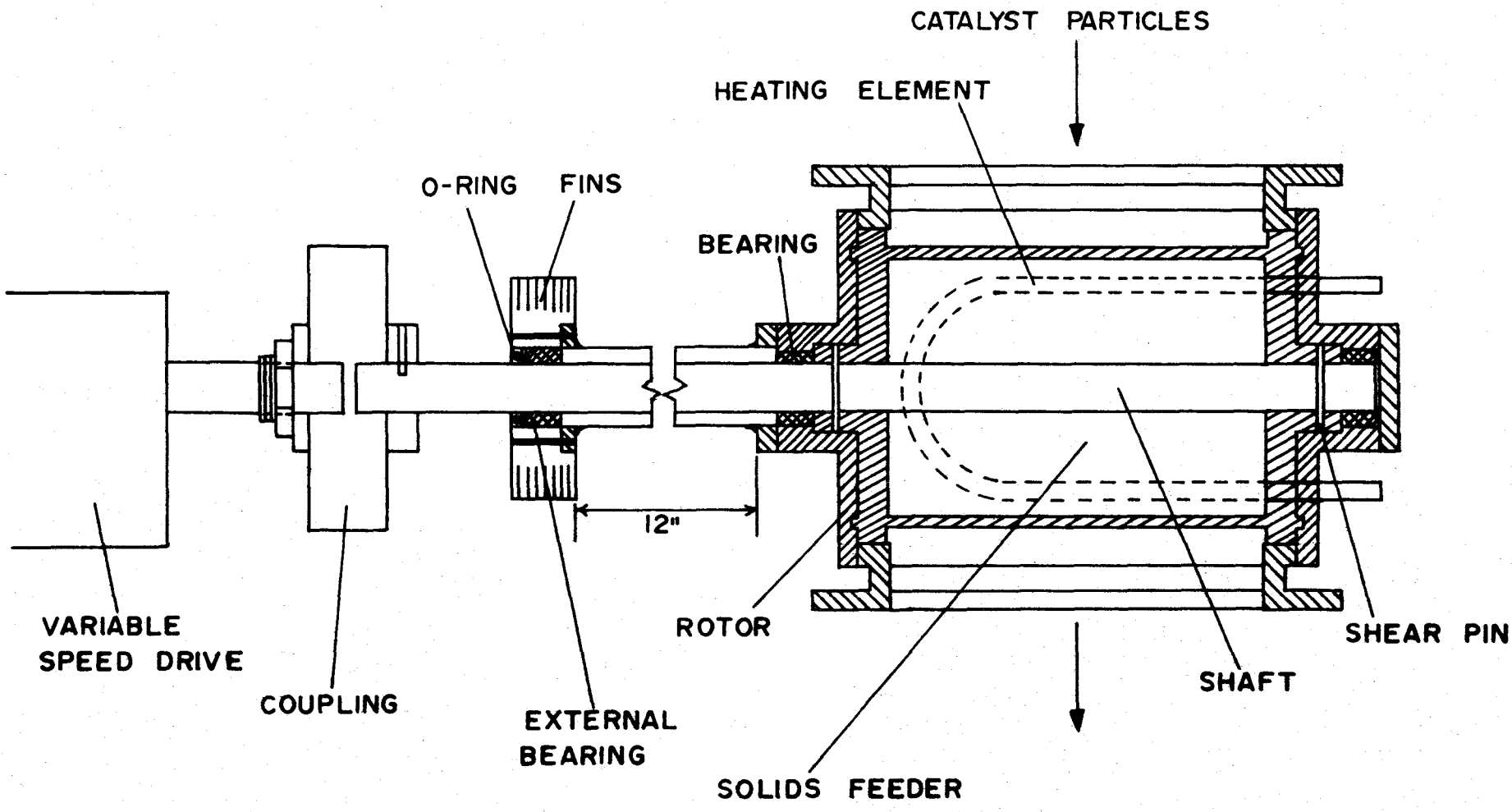

CATALYST FEEDING SYSTEM

The valve rotor was machined from a 6 in. length of 3 1/2 in. schedule 80 stainless steel pipe. Grooves, running parallel to the axis, are machined in the wall of the rotor. These grooves are 0.125 in. x 0.188 in. in cross-section and are machined on 6 degree centers, giving a total of 60. Type 316 stainless steel plates are welded to each end of the rotor. A 3/4 in. stainless steel shaft passes through the center of each endplate. The shaft is fixed to the rotor with a shear pin.

The housing was machined from a 6 in. section of 4 in. diameter schedule 40 stainless steel pipe. The solids entrance and exit ports are welded to the housing. A chromel-alumel thermocouple, made from 1/16 in. Ceramo wire, is imbedded in the wall.

An end plate is bolted to each end of the housing. The purpose of the end plates is to seal the unit and to provide bearings for the shaft. Bearings, made of Bearium high temperature bearing material, are fitted into the center of the end plates.

An o-ring seal is required to make the unit gas tight. This o-ring is located in an external bearing. The seal must be located externally because temperatures adjacent to the valve are too high for a neoprene o-ring. Aluminum fins are press fitted around the external bearing to enhance heat transfer.

The valve shaft is connected to the variable speed drive by a Dalton ROSDC Rigid coupling. This coupling can be adjusted to slip at any desired torque. In practice, the coupling was set to slip at a torque slightly lower than the maximum rating of the variable speed

drive.

Speed control for the valve is provided by a Zero-Max variable speed drive. This unit produces a constant torque (85 in lb. at 0 - 50 rpm) regardless of the speed of rotation or the load.

To reduce the possibility that the rotor will expand much more than the housing and cause binding, heaters are mounted on the outside of the housing. These heaters, Chromalox tubular heating elements, are mounted on each side of the housing. Power input to each unit is 750 watts at 110 volts and is controlled by a powerstat. Insulation is with Hiloset cement.

The valve, except for the coupling and variable speed drive, is insulated with two inches of Thermobestos.

(f) Reactor Coolant System

The components of the reactor coolant system are:

(i) Circulation Pump

(ii) Salt Tank

(iii) Transfer Lines

(iv) Immersion Heaters

The circulation pump is a 1 1/4 in. Class CO vertical cantilever pump with an air-cooled shaft. It has a throughput of 5 USGPM at a head of 20 ft. The pump is specially designed for high temperature operation, the drive shaft being hollow with holes drilled in the wall to draw in air while rotating. All material is carbon steel.

The salt tank is suspended from the base plate of the pump.

The tank is 18 in. I.D. x 19 3/4 in. deep and was fabricated from 1/16 in. stainless steel plate with a 1/4 in. stainless steel bottom plate. The pump impeller extends into the tank to a depth of ten inches. A 50 ft. length of 3/8 in. copper tubing is coiled around the outside of the tank. Steam at 100 p.s.i.g. and 335°F flows through this coil and into a Sarco steam trap. The coil is covered to a depth of approximately one inch with Thermon heat-transfer cement. A 1/16 in. Ceramo chromel-alumel thermocouple is immersed in the salt tank. Heat input to the tank is with six Chromalox immersion heaters screwed to the bottom plate of the tank. Power supply to the heaters is 230 volt, 3 phase and is controlled by powerstats, one for each phase. The heaters, two per phase, are delta connected so that a maximum of 230 volts is available for each heater. Power input per heater at 230 volts is 1100 watts.

Transfer lines to and from the reactor jacket are 3/4 in. x .035 in. wall stainless steel tubing. The line to the jacket contains an 8 in. section of 3/4 in. stainless steel bellows. Salt enters the reactor jacket at the bottom and leaves at the top. The salt return line extends to within one inch of the tank bottom in order to discourage short-circuiting of the salt to the pump impeller. All tube fittings are 3/4 in. stainless steel Swagelok. An 18 in. long 1 1/8 in. diameter stainless steel jacket is located in the salt return line immediately downstream from the reactor jacket. This forms a double-pipe heat exchanger in the salt return line. It was envisaged that air would be passed through this jacket to remove some of the reaction heat from the

salt. However, it became apparent soon after start-up that heat losses from the salt circulation system were more than sufficient to remove the heat of reaction. Hence, this heat exchanger was not used.

The salt transfer lines are steam traced to prevent salt from freezing and causing blockages. Details of the tracing method are identical to those for the reactor and are described in section 5.1.2 (c). Two chromel-alumel thermocouples are located in the salt return line on either side of the heat exchanger. These thermocouples were placed into holes drilled in the salt line and silver-soldered into position.

The reactor coolant system is laid out so that on shut-down all the salt in the system will drain to the tank.

The entire salt circulation system is insulated with two inches of Thermobestos.

(g) O-Xylene Feed System

O-xylene is fed to the carburetor from a brass feed tank. This tank was machined from a 20 in. section of 6 in. nominal diameter brass pipe. The top is flange-connected and sealed with a neoprene o-ring. A sight glass is mounted on the tank. This glass is an 18 in. length of 3/8 in. O.D. x .094 in. wall Pyrex glass, and is connected to the tank with 3/8 in. brass Swagelok fittings with Teflon ferrules. The o-xylene discharge line is silver-soldered to the top flange and with the flange in position extends to within one inch of the tank bottom. Also located in the top flange plate is a connection for the nitrogen cylinder and a 1/4 in. Nupro purge valve.

From the feed tank, o-xylene flows through the following sequence (transfer lines are 1/4 in. copper tubing):

(i) a 1/2 in. Jamesbury Ball Valve - for emergency shutdowns.

(ii) a 1/4 in. Millaflow brass Regulating Valve - This valve is used to set the desired flowrate of o-xylene.

(iii) a rotameter mounted to the control panel with brass Swagelok fittings - A teflon sleeve seals the rotameter fitting.

(iv) a 1/4 in. Whitey Vee-Stem Valve - This valve is located in the line just before the carburetor. Its purpose is to provide back pressure to prevent the o-xylene from bubbling as it flows through the control valve. The metering valve and rotameter are located some twelve feet above the carburetor. As a result, the line from the rotameter to the carburetor empties rapidly, producing bubbles of o-xylene. With a valve at the level of the carburetor, the line can be kept filled and a smoother flow results.

5.2 Analytical

5.2.1 Analysis Equipment

The major part of the analysis was done with a Beckman GC-2A gas chromatograph, equipped with a thermal conductivity detector, and a Fisher Laboratory Integrating Recorder. A 6 ft. x 1/4 in. O.D. stainless

steel column packed with Chromosorb W 60/80 mesh and coated with 25% Dow Corning Silicone oil plus 2% phosphoric acid was used separate the components.

Chromatograph conditions were as follows:

Column Temperature: 486°F (252°C)

Carrier Gas: Helium

Carrier Gas Flowrate: 106 c.c./min. at atmospheric pressure and ambient temperature

Filament Current: 250 ma.

Sampling Valve Temperature: 295°F (146°C)

The maximum retention time under these conditions was ten minutes.

Sample injection into the chromatograph was accomplished with a Carle Instruments Inc. gas-sampling valve. Figure 7 is a schematic diagram of the sampling system. The sampling valve consists of two matched stainless steel loops of 1.0 ml. volume with a switching arrangement so that the flow of sample and carrier gas can be switched from one loop to another.

Sample flows from the cyclone separator through a Gelman stainless steel filter holder with a glass fiber filter. The filter has an efficiency of 99.7% for particles larger than 0.2 micron. From the filter the sample flows through one loop of the sampling valve. Carrier gas flows through the other loop and into the chromatograph column. When the valve is switched, carrier gas flows through the loop through which sample had been flowing and the sample flows through the

other loop. This causes a precise volume of sample gas to be injected into the chromatograph as a slug.

The temperature of the gas sampling valve is controlled manually by electrical heaters. An aluminum thermal compartment encloses the entire valve. The outside of the compartment is wrapped with nichrome wire insulated from the walls with Hiloset refractory cement (Kaiser Refractories Co.). Power input at 110 volts is 100 watts.

The temperature of the compartment is measured by copper-constantan thermocouples mounted adjacent to the sample loops and is controlled by a powerstat. The sample line is 1/8 in. stainless steel tubing and is heated by electrical heating tape.

A water aspirator controls the pressure in the sample system. The pressure of the sample at the time the valve is switched is taken as the difference between atmospheric pressure and the aspirator pressure. A manometer indicates this pressure difference.

Some samples were analyzed by Nuclear Magnetic Resonance (NMR) spectroscopy. The instrument used for these analyses was a Varian Model A-60 NMR Spectrometer System.

Measurement of catalyst particle size distribution was made by microscopic methods. Photographs of the catalyst samples were taken at a magnification of 90 and the images of the individual particles were counted and classified with a Carl Zeiss type TGZ 3 Particle Size Analyzer.

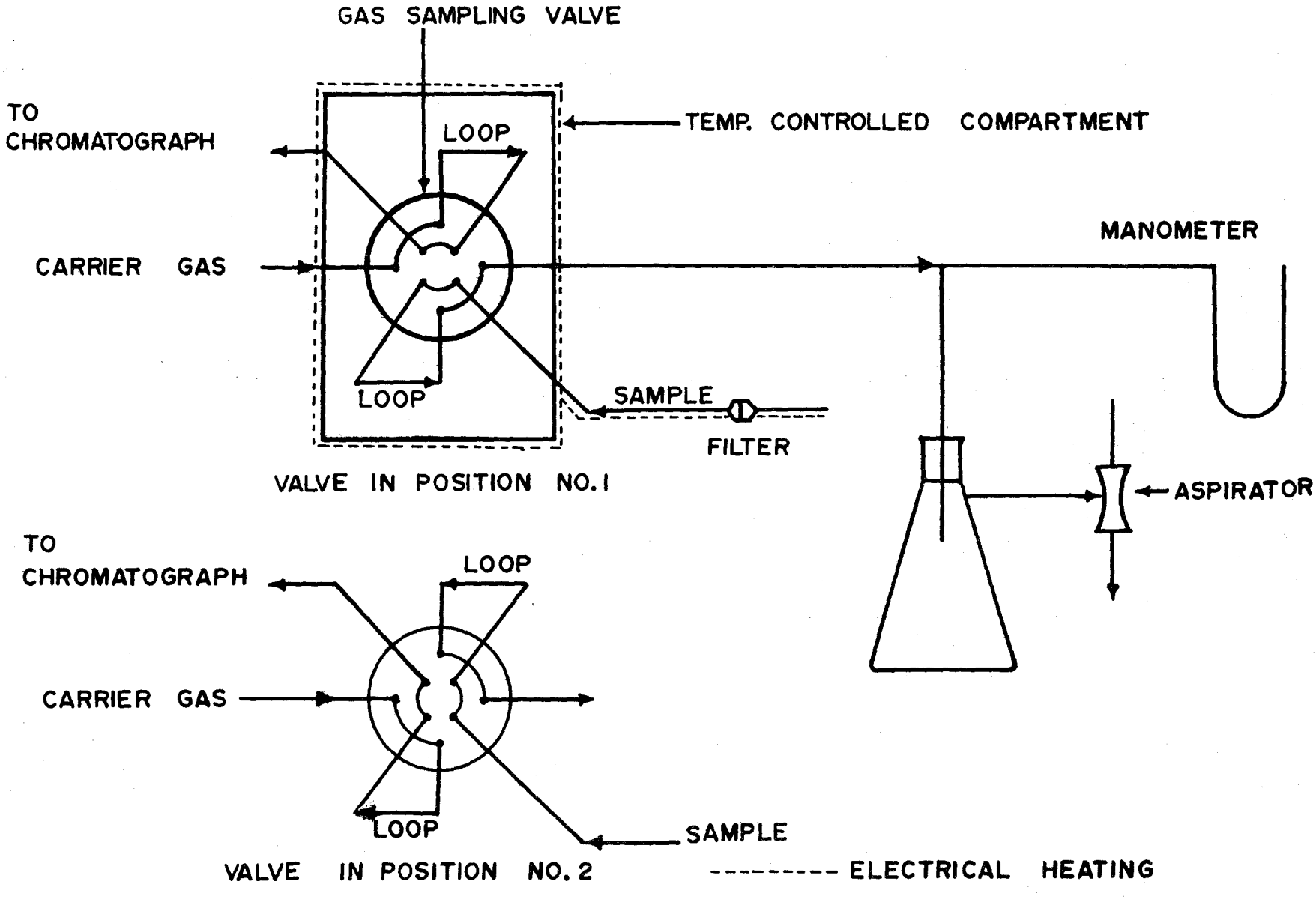
GAS SAMPLING VALVE
TO CHROMATOGRAPH
LOOP
TEMP. CONTROLLED COMPARTMENT
MANOMETER
CARRIER GAS
LOOP
SAMPLE
FILTER
ASPIRATOR
VALVE IN POSITION NO. 1
TO CHROMATOGRAPH
LOOP
CARRIER GAS
LOOP
SAMPLE
VALVE IN POSITION NO. 2
--------- ELECTRICAL HEATING

5.2.2 Analyses Carried Out

(a) Reactor Effluent Stream

The gas stream discharging from the reactor was analyzed periodically with the gas chromatograph. This analysis provided the quantitative data necessary to evaluate the kinetic parameters of the system and to identify the products. Section 5.2.1 outlines the sampling method used. The chromatograph functioned as an on-stream analyzer. The reactor effluent stream was monitored continuously and an instantaneous sample could be taken at any desired time.

(b) Reactor Condensate

The stream discharging from the water-cooled trap contained condensate. This condensate was collected and analyzed by gas chromatography and NMR spectroscopy. This analysis was qualitative in that no attempt was made to collect all the condensate over a measured period of time. Product identification was the sole object. Liquid samples were injected into the chromatograph with a Hamilton microlitre syringe. Condensate samples were vacuum distilled and the distillate was used for the analytical work.

(c) Catalyst Particle-Size Distribution

Measurements of catalyst particle size distribution were made on samples of fresh catalyst and on samples obtained after twenty hours of use. Section 5.2.1 outlines the method. The size distribution of fresh catalyst is based on a sample of 3000 particles; the used catalyst on a 2700 particle sample. Size-distribution analyses were made

in order to characterize this particular catalyst and to estimate the amount of catalyst attrition that had occurred.

To further characterize the catalyst, a surface area measurement was made based on the theory of Brunauer, Emmett, and Teller (55). This theory relates the surface area of the catalyst to the amount of nitrogen adsorbed at its boiling point. A description of the theory as well as the experimental apparatus is given in the book by Ross and Olivier (56).

5.2.3 Calibration

The gas chromatograph was calibrated by injecting liquid samples of known composition and measuring the recorder response. For o-xylene and maleic anhydride, the response measured was peak height, while it was necessary to measure peak areas for o-tolualdehyde and phthalic anhydride. The latter two compounds exhibited rather broad peaks with some tailing. Peak areas were measured by following the recorder trace with a #31 Ott Planimeter.

Standard solutions of each component to be calibrated were prepared with acetone as the solvent. Acetone is an excellent solvent for this work because its retention time in the chromatograph is so short that its peak does not interfere with the component peak of interest. It was found that MIBK instead of acetone as the solvent did not affect the retention times of the component peaks. Acetone was employed, however, because solubilities were higher. Solutions of 0.5, 1.0, and 2.0 weight % component in acetone were prepared for o-xylene, maleic anhydride, o-tolualdehyde, and phthalic anhydride.

Samples of 1.0, 2.0, and 3.0 µl of each of these solutions were injected into the chromatograph with a Hamilton microlitre syringe. This procedure resulted in nine different pairs of gm. mole. - peak height (area) points for each component. A reproducibility among equal volume injections of the same sample of $\pm$ 1.5% could be obtained by syringe injection.

5.2.4 Catalyst

The catalyst used for this work was a V_2O_5 - K_2SO_4 - silica gel catalyst donated by the American Cyanamid Company. An exact chemical analysis could not be obtained but, based on two patents granted for the preparation of this type of catalyst (42, 43), an approximate composition is given below.

COMPOUND	% BY WEIGHT	FUNCTION
V_2O_5	9 - 11	Active Catalytic Ingredient
K_2SO_4	30 - 40	Stabilizer
S_iO_2	40 - 55	Support
Oxides of Metals from group III-B or IV-A of the Periodic Table	Trace	Promoter

The catalyst, as received, exhibited a large size range (10 - 400 microns). In order to reduce this range and to minimize the slip velocity between the catalyst particle and the gas stream in the reactor, only the −100 mesh fraction was used in this study. The catalyst was screened through

a 100 mesh Tyler sieve with a mechanical shaker.

Additional properties of the catalyst are listed below:

Size Distribution: Figure 8

Bulk Density: 39 lb./cu. ft.

True Density of Solid: 131 lb./cu. ft.

Average Diameter (Surface Average): 48.1 microns (0.00189 in.)

Surface Area (obtained by BET Measurement): 170.6 sq. M/gm.

Shape: Photographs at a magnification of 90 showed that the particles were very nearly spherical

Colour: Olive Green

5.2.5 Chemicals

(a) O-Xylene

Analytical Work:

Supplier: Matheson Coleman and Bell

Cat. No.: XX 17

Grade: Chromatoquality Reagent

Purity: 99 + mole %

Reactor Feed:

Supplier: Eastman Organic Chemicals Ltd.

Grade: Highest Purity

Melting Point: − 25°C to − 23°C

(b) Phthalic Anhydride

Supplier: Baker Chemical Co.

Cat. No.: 0272

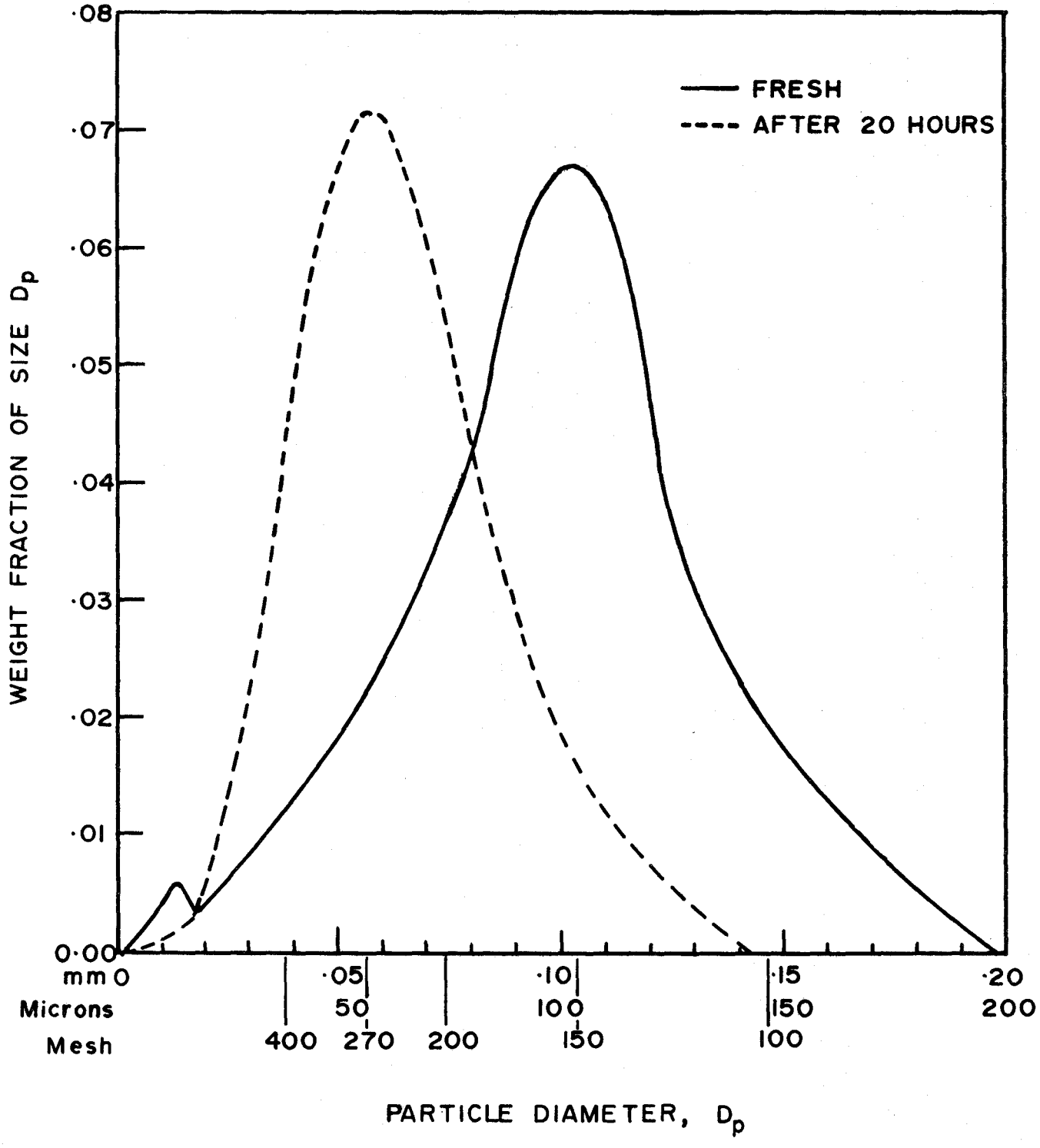
·08
·07
·06
·05
·04
·03
·02
·01
0·00
FRESH
AFTER 20 HOURS
WEIGHT FRACTION OF SIZE D_p
mm 0
·05
·10
·15
·20
Microns
50
100
150
200
Mesh
400
270
200
150
100
PARTICLE DIAMETER, D_p

Grade: Reagent

Melting Point: 129°C - 131°C

Maximum Impurity: 0.009%

(c) Maleic Anhydride

Supplier: Matheson Coleman and Bell

Cat. No.: MX 113

Grade: Reagent

Melting Point: 53°C - 55°C

(d) O-Tolualdehyde

Supplier: Matheson Coleman and Bell

Cat. No.: TX 720

Grade: Practical

Boiling Point: 197°C - 199°C

5.3 Experimental Procedure

5.3.1 Start-Up

Before beginning a run, the solids hold-up tank was filled to a depth of 3 ft. 6 in. with fresh catalyst and the o-xylene feed tank was filled. A "head" of catalyst of at least 3 ft. 6 in. above the solids feeder appeared to be necessary in order to minimize the flow of reactant gases upwards through the solids hold-up tank instead of through the reactor. The magnitude of the flow of gases through the solids hold-up tank was not measured. The preparation of the fresh catalyst is described earlier. After filling the o-xylene feed tank, the air above the o-xylene was purged with nitrogen. The tank was always blanketted

with nitrogen.

Approximately ten hours prior to start-up, power was turned on to the solids hold-up tank heaters and to the fused salt tank heaters. The apparatus was always left with the steam tracing on. This maintained the contents of the fused salt tank in a molten state and at a temperature of approximately 330°F. After the heating-up period (when the interior of the solids hold-up tank and the fused salt tank had reached about 400°F and 550°F respectively) the air flow was started and power was supplied to the electrical heaters of the carburetor and reactant preheater. When the temperature of the air discharging from the preheater reached a minimum of 400°F, the fused-salt circulation pump was switched on. At a preheater discharge temperature of less than 400°F, the salt would freeze in the reactor jacket despite the steam tracing on the outer surface. Salt circulation could be easily confirmed by the thermocouples in the salt return line. If salt was circulating, the temperature in the salt return line immediately jumped to the temperature of the salt tank: if there was a block in the reactor jacket, the temperature in this line remained equal to the temperature of steam in the tracing system, i.e., 330°F.

As soon as a steady air flow was established, the solids feeder was started at about 25 rpm. When the solids feeder was running, auxiliary air flow was begun, directing two diametrically opposed jets of air at the catalyst stream just as it entered the solids discharge cone.

The auxiliary air flow prevented the solids from bridging in the cone. Without this air flow, the catalyst would back up in the cone and jam the solids feeder. In the initial stages of the work, a vibrator apparatus was installed on the solids discharge cone. The vibrator did not have a visible effect on the rate of solids flow. Its use was therefore discontinued.

Power was supplied to the electrical heaters mounted on the housing of the solids feeder at a rate such that the temperature of the wall of the housing was always slightly higher than the temperature of the catalyst flowing through the feeder. This reduced the possibility of the feeder jamming because of unequal expansion of the rotor and housing.

Once the solids feeder was functioning smoothly, it was necessary to wait about seven hours for the system to come up to the reaction temperature of 750°F with the solids hold-up tank heaters at 24 volts, and the carburetor and preheater set at 17.5 volts. It was found that with full power on the salt tank heaters the temperature of the salt-circulation system would level off at about 700°F. Therefore, in order to operate at a reaction temperature of 750°F, it was necessary to supply heat to the system via the solids hold-up tank heaters and to stop salt circulation. This procedure caused a temperature difference between the top and bottom of the reactor of about 20°F. This was because without salt circulating in the reactor jacket, the gas-solids mixture lost heat as it flowed up the reactor. Such a temperature drop

is avoided when salt is circulating because the heat capacity of the flowing salt is so great that both the solids and gas temperatures rapidly become equal to the salt temperature.

Approximately five hours before the system came to steady state, the chromatograph and associated analytical equipment was started. This was accomplished by turning on the carrier gas to the chromatograph and electric power to the column thermal compartment and sampling valve thermal compartment heaters. Temperatures of each sample loop of the gas-sampling valve and of the column thermal compartment were continuously monitored with a Philips 12 point recorder. It required approximately one hour for the temperatures to reach steady values so that the chromatograph was well conditioned before samples were analyzed.

5.3.2 Steady-State Operation

When steady-state temperatures were attained, o-xylene was fed to the reactor. A few minutes after the commencement of o-xylene feed, the temperature of the air : o-xylene mixture leaving the carburetor began to drop rapidly. This occurred because of the sensible and latent heat required to bring the o-xylene to the vapour state. When the carburetor exit temperature levelled off, samples of reaction products were taken and analyzed. Some difficulty in maintaining a steady flow of o-xylene was encountered. From time to time slugs of vapour would appear in the o-xylene rotameter. These slugs were attributed to dissolved nitrogen coming out of solution as the o-xylene flowed through

the diaphragm control valve. The problem was reduced, though not eliminated completely, by installing a needle valve in the o-xylene line just before the carburetor. This increased the back pressure in the o-xylene feed line and reduced slugging.

In preparation for taking a sample, the water aspirator was set so that a vacuum of about fourteen inches of water was created in the sample system. Figure 7 shows a schematic representation of the sampling set-up. Such a vacuum was necessary because the reactor pressure at the sample point (≈8" H_2O) was insufficient to force a significant flow of sample through the filter.

A sample was taken by simply switching the gas sampling valve. The signal from the chromatograph was recorded with a Fisher Laboratory Integrating Recorder. Figure 10 shows a typical chromatogram. At least ten minutes was allowed before taking a new sample so that no peaks would be missed. Whether or not the reactor was operating at steady-state was judged by the consistency of successive chromatograms. When the chromatograms of two successive samples were nearly identical, steady-state conditions were considered to be achieved and the reaction conditions were changed to a new set. The nearly identical chromatograms were used for product analysis at that particular reaction condition.

Some care had to be exercised to prevent too high a preheater discharge temperature. If the temperature became higher than about 1100°F, complete combustion would occur and large heat effects would result.

Even though the preheater temperature reached such high values, the remainder of the apparatus was not endangered because as soon as the hot gases met the catalyst stream, the temperature of the mixture immediately dropped to a safe level. The heat capacity of the solids relative to the gas is so large that a considerable amount of heat can be transferred from the gas without increasing the solids temperature appreciably. Consequently, during normal operation the heat of reaction could be absorbed by the gas-solid mixture while still maintaining isothermal conditions. During periods of complete combustion in the preheater, the temperature of the gas-solid mixture did rise about 100°F but not to a dangerous level.

So long as the temperature of the gas mixture discharging from the preheater was kept below about 1100°F the reaction was stable; if the temperature was allowed to rise much above 1100°F, the reaction was unstable, and a runaway reaction would occur.

5.4 Experimental Difficulties

This section describes some of the experimental problems that were encountered in the thesis investigation. A brief description of the development work necessary to solve these problems is also included.

5.4.1 Catalyst Feeding

The development of a satisfactory method of feeding the catalyst into the gas stream posed the major problem. The high feeding temperature complicates the situation, creating difficulties in lubricating

the bearings of the rotary feeder and of sealing the catalyst particles from the bearings.

Initially, the solids feeder was operated at room temperature. After only a few minutes of operation, the rotor jammed. This was traced to a build-up of catalyst in the solids discharge cone, i.e., the gas stream was not removing the solids as fast as they were being discharged by the feeder. The resulting accumulation of catalyst packed the space between the feeder rotor and housing, causing the rotor to jam. When the rotor jammed, the clutch connecting it to the variable speed drive slipped and the flow of solids ceased.

Two alterations to the system were made to overcome the problem. First, an air line to the cone was installed which directed two jets of air at the solids stream just as it left the feeder. This effected a pronounced improvement in solids feedrate. The stream of air probably prevented the solids from bridging in the cone. Initially, a vibrator was mounted to the discharge cone to prevent bridging. However, vibration had little or no effect on the solids feedrate. The second measure taken to improve solids feeding was to operate the system with a larger inventory of catalyst in the solids hold-up tank. The combination of air jets to the cone and larger catalyst inventory completely eliminated the catalyst build-up problem at room temperatures.

It was concluded that catalyst accumulation was caused by part of the gas mixture by-passing the reactor and flowing upward through the solids hold-up tank. The upward air flow through the discharge cone

impeded the downward flow of catalyst. With a higher "head" of solids above the feeder the resistance to flow through the bed was increased and the upward air flow decreased. The result was an increase in the amount of catalyst that discharged into the gas stream.

When operation of the solids feeder at higher temperatures was attempted, the rotor again jammed frequently, even though the catalyst build-up problem had been eliminated. This time the jamming was attributed to unequal thermal expansion of the rotor and housing and to the presence of catalyst in the bearings of the rotor. When the feeder was disassembled after jamming, it was found that the catalyst had worked its way into the space between the bearings and the shaft. Also, the lubricant (Molyslip graphite type) had vapourized, leaving a film on the shaft. When the catalyst was removed from the bearings and fresh lubricant applied, the rotor again turned freely. Some improvement in the operation of the feeder at higher temperatures was achieved by heating the housing and by using flake graphite as a lubricant. The feeder then operated well enough for this study although the bearings squealed loudly and several times the feeder jammed temporarily.

Because of the high temperatures involved, it was not possible to provide a seal on the rotor shaft between the rotor and the bearings. With a seal, catalyst could be kept out of the bearings and operation would be smoother.

5.4.2 Catalyst Attrition and Loss

Excessive carryover of catalyst from the cyclone was another

problem. Catalyst carryover is undesirable because apart from the loss of catalyst, it fouls the cold trap and the gas exhaust line. On one occasion a mixture of catalyst and hydrocarbons completely plugged the exhaust line. During a twenty-hour period of continuous operation, approximately 16% of the catalyst originally charged to the solids hold-up tank was lost.

An indication of catalyst attrition can be obtained by considering the weight-size distribution of fresh catalyst and catalyst after twenty hours of operation. These curves are shown on Figure 8. It is apparent that the curve for used catalyst has shifted to the left. This shift means that the weight average particle size has decreased because of catalyst attrition. The effect of catalyst carryover can also be seen from Figure 8 . The curve for the fresh catalyst has a larger fraction of fine particles (less than 20 microns) than the used catalyst curve. Therefore, a portion of the fines has been lost from the system.

It is of interest to note that despite the attrition, the surface average diameter, defined as the diameter of a sphere whose surface multiplied by the total number of particles in the sample equals the total surface area of the sample, has actually decreased from 48 microns to 45 microns. This is because two effects are present: attrition, which increases the surface area, and carryover, which reduces the surface.

It was observed that carryover was most severe in the initial

part of the run. It would therefore appear that once the fines originally present are eluted from the system, losses level off. After the start-up period, fines created by attrition would be lost. The observation noted above indicates that these losses are small.

Some carryover of fines from the cyclone is to be expected. The separation efficiency of a cyclone, defined as the percentage of particles of a given size removed from the gas stream, decreases with decreasing particle size. Figure 9 shows an efficiency curve for the cyclone used in this study. It is seen that for particles smaller than 10 microns, the separation efficiency decreases rapidly. The cyclone was designed according to the high efficiency design proposed by Stairmand (52), the efficiency curve being derived from his work.

A major cause of entrainment and carryover is thought to be the pickup of particles which have already been separated (52). A central vortex, through which the dust-free gas leaves the cyclone, extends into the solids receiver. Some of the solids in the receiver are entrained by this vortex and carried out with the gas.

It is felt that the entrainment phenomenon described above is not a factor in this system. The basis for this belief is that operation with a rotary valve between the cyclone and the solids hold-up tank did not reduce carryover. Initially, the system contained two identical rotary valves; one to feed the solids into the gas stream and one to discharge the catalyst from the cyclone. When the top valve was taken out of the system because of jamming problems, the performance of the

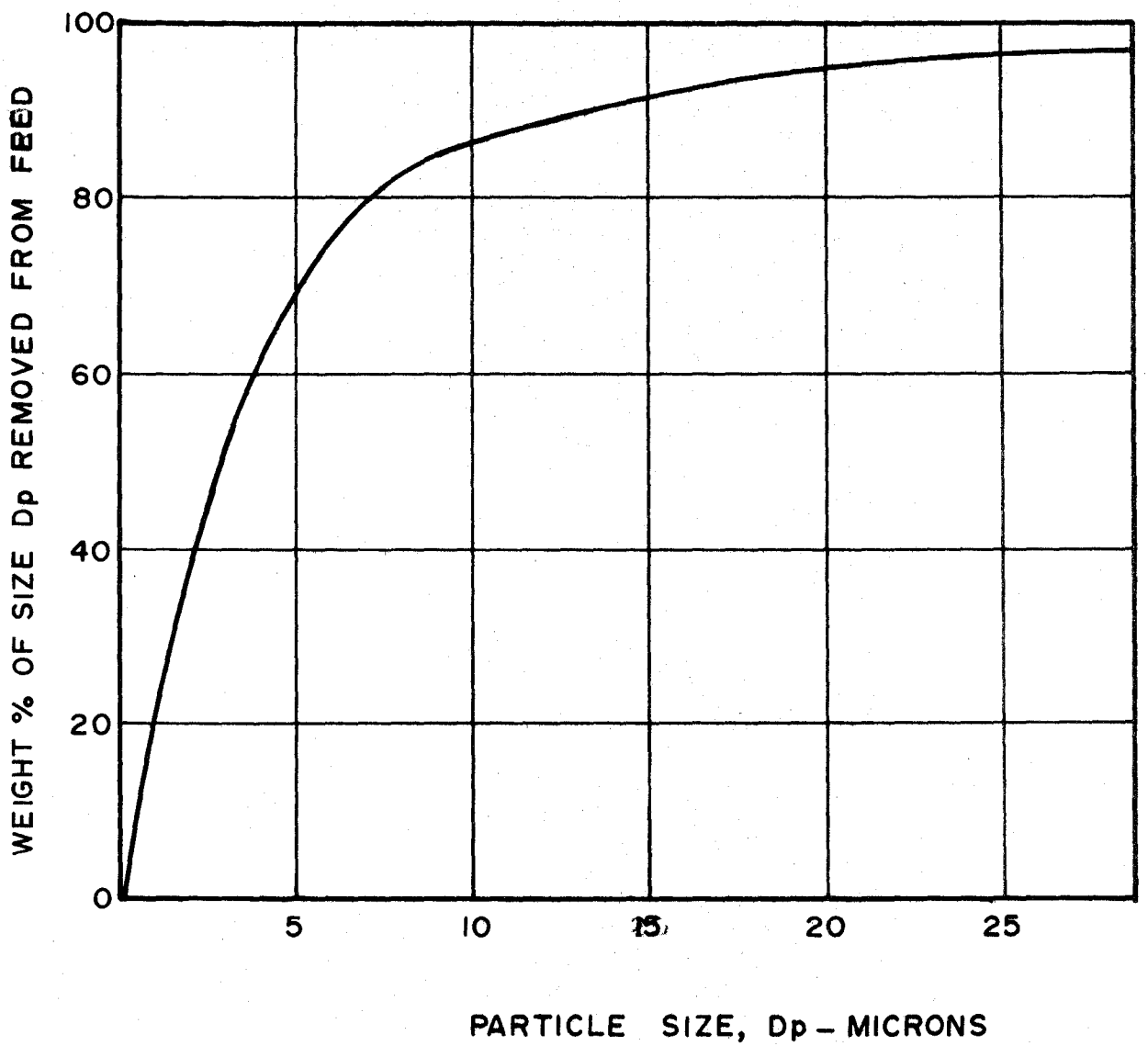
100
80
60
40
20
0
WEIGHT % OF SIZE Dp REMOVED FROM FEED
5
10
15
20
25
PARTICLE SIZE, Dp – MICRONS

cyclone improved. This would not be expected if vortex-entrainment was occurring because the rotary valve should prevent the vortex from entering the solids hold-up tank and hence improve the separation. The opposite effect was observed.

5.5 Experimental Program

The data for this investigation were obtained from one series of experiments in which the air feedrate and reaction temperature were constant. Because a large excess of air was used, the variation in o-xylene feedrate had little effect on the total gas feedrate. Hence the space time was essentially constant.

Variables investigated were o-xylene feedrate and catalyst feedrate. Values of o-xylene feedrate studied were 0.85, 1.16, and 1.81 lb./hr. Catalyst feedrates of 186, 340, 355, 439, and 492 lb./hr. were investigated.

A number of samples were taken and analyzed for various combinations of o-xylene feedrate and catalyst feedrate.

In actual fact the reaction temperature varied slightly during the experiments. This variation was small. In the calculation of conversion, a correction is made for temperature changes.

6. RESULTS

This section summarizes the experimental results in terms of the products of the reaction and the kinetic behaviour of the reactor. Product identification is based on gas-chromatographic analysis of gas samples taken during the course of the reaction and on gas chromatographic and NMR analysis of liquid samples of condensate collected from the cold trap at the end of the run. Kinetic data are obtained only from gas sample analyses.

Appendix 1 includes a complete listing of both the measured and calculated experimental data. It also illustrates the calculation procedure with a sample calculation.

6.1 Product Identification

Figure 10 shows a typical chromatogram of a gas sample. The recorder response, expressed as a percentage of the full chart scale, is plotted on the ordinate versus the retention time, i.e., the elapsed time since the sampling valve was switched, on the abscissa. Chromatograph operating conditions for all samples were:

Column: 6 ft. x 1/4 in. O.D. S.S. tubing packed with 25% Silicone Oil + 2% Phosphoric Acid on 60/80 Mesh Chromosorb W

Column Temperature: 252°C (450°F)

Filament Current: 250 ma.

Carrier Gas (Helium) Flowrate: 106 cc./min.

Sampling Valve Temperature: 145°C (295°F)

Sampling Valve Pressure: 11 in. water vacuum

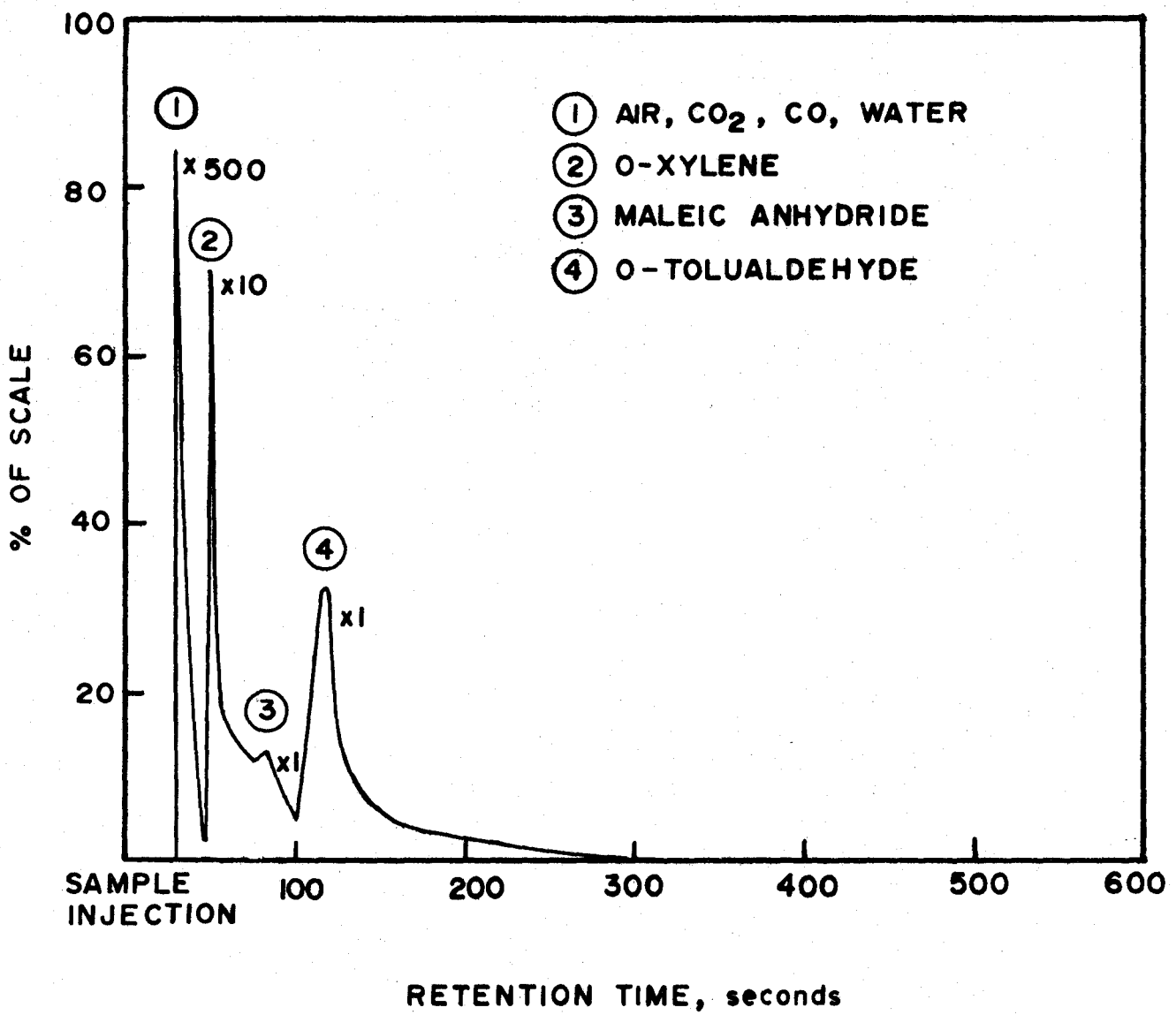
100
80
60
40
20
% OF SCALE
① AIR, CO_2, CO, WATER
② O-XYLENE
③ MALEIC ANHYDRIDE
④ O-TOLUALDEHYDE
x500
x10
x1
x1
SAMPLE INJECTION
100
200
300
400
500
600
RETENTION TIME, seconds

Peak 1 represents the non-hydrocarbon components of the sample. These are unreacted air plus small amounts of carbon dioxide, carbon monoxide and water formed from complete oxidation reactions. Since the reactor feed contains a large excess of air, the contribution of these complete combustion products to the height of the peak is insignificant. Peak 1 was identified by comparing retention times with samples taken when air only was being fed to the reactor. Retention times were identical (28 seconds).

Peak 2 is the unreacted o-xylene peak. This was established by comparing retention times with samples of chromatographic grade liquid o-xylene injected with a microlitre syringe under identical chromatograph conditions. The retention time (to maximum peak height) was 52 seconds in each case.

Peak 3, although too small to analyze quantitatively, appeared consistently at a retention time of 77 seconds. The peak was concluded to be due to maleic anhydride (MA) by virtue of identical retention time of MA in liquid samples of a 3% solution of MA in acetone.

The last compound to be eluted was o-tolualdehyde (OTA). This appears as peak 4. The OTA was confirmed by equal retention time (110 seconds) to that of OTA in a 3% solution in acetone under identical chromatograph conditions. Also, the characteristic odour of OTA could be readily detected during the reaction.

No peaks, other than the four described, appeared in any of the gas samples for any reaction conditions.

A much different chromatogram resulted from analysis of samples of condensate collected from the cold trap at the end of a run. Figure 11 illustrates a typical chromatogram of a condensate sample. Three peaks appear on this chromatogram which do not appear on the chromatogram of a gas sample. These are o-toluic acid (peak 4), phthalic anhydride (peak 5), and phthalide (peak 6). Possible reasons that these compounds were detected in the condensate sample and not in the gas sample are:

(a) Difference in sample size -

The gas samples were 1 ml., while the condensate samples were 5 microlitres (approximately equivalent to 5 ml. of gas). About 95% of the gas sample consists of air. Therefore, the ratio of hydrocarbons in the condensate sample to hydrocarbons in the gas sample is approximately 100.

(b) A change in composition of the gas occurs when it is partially condensed. The condensate becomes richer in the less volatile compounds. Hence the concentration of the high boiling point components would be higher in the condensate than in the reactor discharge stream. The three compounds (peaks 4, 5, and 6) that are detected in the condensate but not in the gas stream have relatively high boiling points as shown by the following table.

TABLE 2

BOILING POINTS OF REACTION COMPONENTS

Peak No.	Compound	B.P. (°C)
1	Acetone	57
2	O-Xylene	144
3	O-Tolualdehyde	196
4	O-Toluic Acid	259
5	Phthalic Anhydride	285
6	Phthalide	290

Referring to Figure 11, the o-xylene, o-tolualdehyde, and phthalic anhydride peaks were identified by comparing retention times with standard samples. The NMR spectrum of condensate samples showed three sharp peaks and one broad peak. By comparing the peak positions with published data, the sharp peaks were identified as o-xylene, o-tolualdehyde, and o-toluic acid. The broad peak was concluded to be due to phthalic anhydride and phthalide. Resolution by NMR spectroscopy of aromatic compounds in which adjacent carbons have oxygen-containing groups attached is poor; hence the broad peak for phthalic anhydride and phthalide.

Further confirmation of peaks 5 and 6 can be obtained by comparing the chromatogram of Figure 11 to the chromatograms published by Mann (37) and Loftus (26, 27). Mann, analyzing o-xylene oxidation

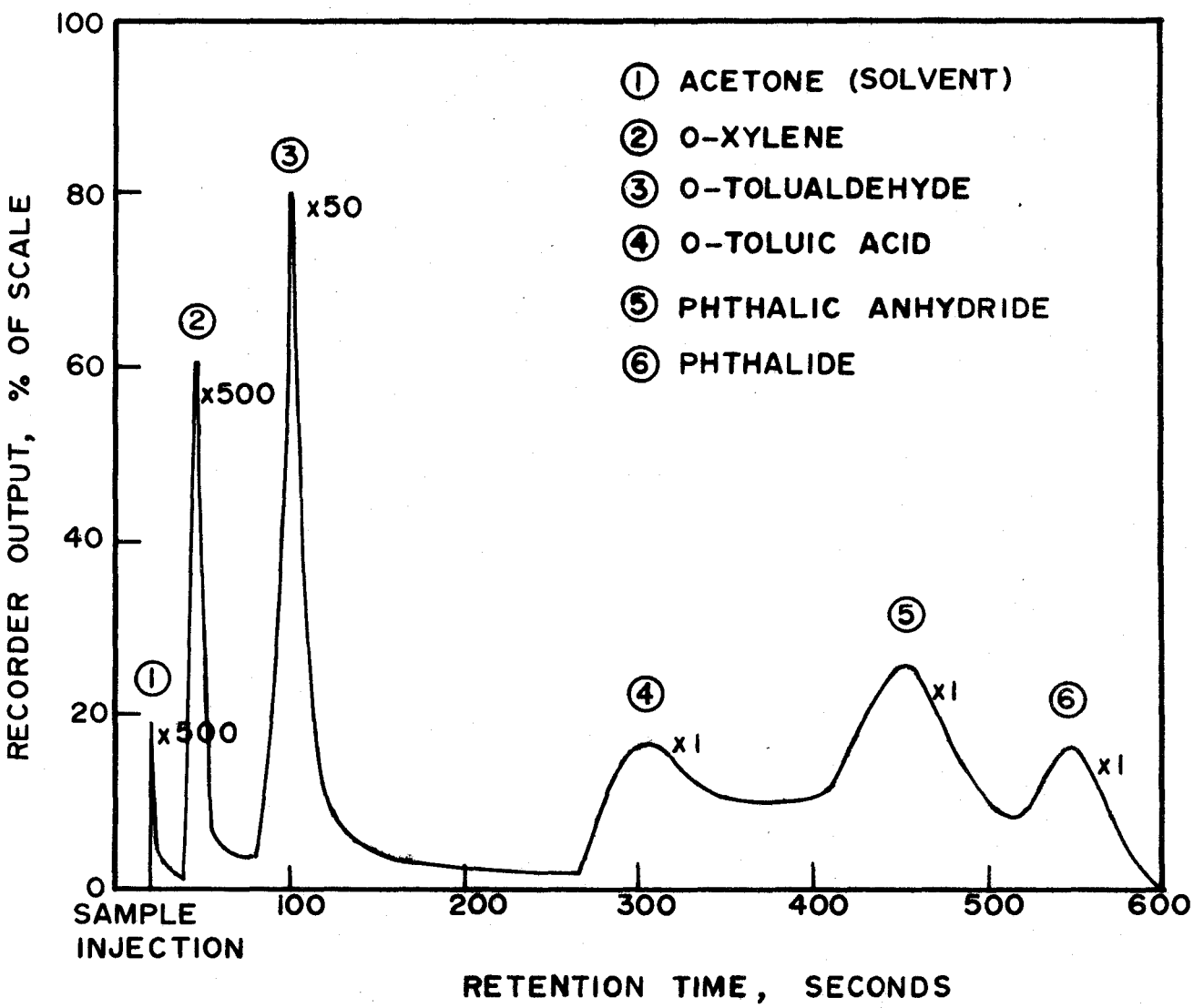
100
80
60
40
20
0
RECORDER OUTPUT, % OF SCALE
① ACETONE (SOLVENT)
② O-XYLENE
③ O-TOLUALDEHYDE
④ O-TOLUIC ACID
⑤ PHTHALIC ANHYDRIDE
⑥ PHTHALIDE
①
x500
②
x500
③
x50
④
x1
⑤
x1
⑥
x1
SAMPLE INJECTION
100
200
300
400
500
600
RETENTION TIME, SECONDS

products on a silicone gum rubber column, found that the phthalide peak was eluted immediately after the phthalic anhydride peak. The same order of elution, phthalic anhydride followed immediately by phthalide, was observed by Loftus who carried out the analysis of o-xylene oxidation products with silicone vacuum grease as the partitioning agent.

The identification of maleic anhydride as a reaction product in this study could be questioned. Peak 3 on Figure 10 was identified as maleic anhydride on the basis that it was eluted at the same time as maleic anhydride in a 3% solution in acetone. However, maleic anhydride did not appear in either gas chromatographic or NMR analysis of the condensate. It is not known why maleic anhydride would appear in the gas sample and not in the condensate sample.

6.2 Treatment of Data

6.2.1 Assumptions

The following assumptions were made in analyzing the kinetic data:

(a) The mass of catalyst per unit volume of reactor is constant throughout the reactor. This requires that the solids be in plug flow.

(b) The gas flow is fully turbulent. This assumption is valid because the Reynolds Number for this study is 5600.

(c) The volume change on reaction is negligible. For this to be true, the reaction must be isothermal, the pressure drop across the reactor must be negligible, and the total moles of reactants plus products must be constant. All these conditions apply to this work.

(d) The relative velocity between gas and solids, i.e., the slip velocity, is negligible compared to the gas velocity. Normally, the slip velocity is taken as the terminal free-fall velocity of the solid particles. The terminal free-fall velocity of the largest catalyst particles (140 microns) is 2 ft./sec., while the minimum gas velocity is 60 ft./sec.

6.2.2 Material Balance

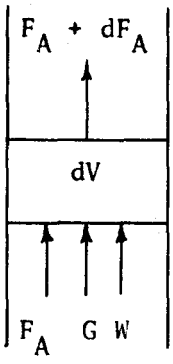

The material balance on o-xylene for a differential volume, dV, of the reactor is:

Input = Output + Disappearance by Reaction

or, $F_A = F_A + dF_A + (-r_A)dW$ (1)

where F_A = Rate of o-xylene entering dV, lb.-moles/hr.

$(-r_A)$ = rate of consumption of o-xylene $\frac{\text{lb.-moles}}{(\text{hr.})(\text{lb.catalyst})}$

dW = Mass of catalyst in section dV, lb.

In section dV, weight of gas = $\varepsilon\ \rho_G\ dV$ (2)

and weight of solids, $dW = (\frac{W_s}{G})\ \varepsilon\ \rho_G\ dV$ (3)

Here, ε = reactor voidage = $\frac{\text{volume of voids (gas)}}{\text{volume of voids (gas) + volume of solids}}$

ρ_G = Density of gas, lb./ft.^{3}

W_s = Flowrate of catalyst, lb./hr.

G = Flowrate of gas, lb./hr.

The reactor voidage, ε, can be found from equations (2) and (3):

$$\text{volume of gas} = \epsilon \, dV \tag{4}$$

$$\text{volume of solids} = \left(\frac{W_s}{G}\right) \frac{\epsilon \, \rho_G \, dV}{\rho_s} \tag{5}$$

where ρ_s = true density of catalyst, lb./ft.^{3}

$$\epsilon = \frac{1}{1 + \left(\frac{W_s}{G}\right) \frac{\rho_G}{\rho_s}} \tag{6}$$

Now, from equations (3) and (6),

$$dW = \frac{\left(\frac{W_s}{G}\right) \rho_G \, dV}{1 + \left(\frac{W_s}{G}\right) \frac{\rho_G}{\rho_s}} \tag{7}$$

Substituting equation (7) in equation (1),

$$-dF_A = \frac{(-r_A) \left(\frac{W_s}{G}\right) \rho_G \, dV}{1 + \left(\frac{W_s}{G}\right) \frac{\rho_G}{\rho_s}} \tag{8}$$

In terms of conversion at any point in the reactor,

$$-dF_A = F_{Ao} \, dX_A \tag{9}$$

where F_{Ao} = Molar feedrate of o-xylene at reactor inlet, lb.moles/hr.

X_A = conversion of o-xylene, $\frac{\text{moles consumed}}{\text{mole fed}}$

Substituting equation (9) in equation (8) and integrating gives:

$$\frac{(\frac{W_s}{G})\ \rho_G\ V}{F_{Ao}\ [1 + (\frac{W_s}{G})\ \frac{\rho_G}{\rho_s}]} = \int_o^{X_{Af}} \frac{dX_A}{(-r_A)} \qquad (10)$$

where X_{Af} = Conversion at reactor outlet

Equation (10) is the design equation for this reactor based on the assumptions discussed in section 6.2.1.

The conversions obtained in this work are always less than 17%; therefore, the reactor can be considered as a differential reactor, i.e., the reaction rate throughout the reactor can be considered constant if isothermal conditions prevail (1).

Then equation (10) becomes (letting X_A equal the conversion in the reactor discharge stream)

$$\frac{(\frac{W_s}{G})\ \rho_G\ V}{F_{Ao}\ [1 + (\frac{W_s}{G})\ \frac{\rho_G}{\rho_s}]} = \frac{X_A}{(-r_A)}$$

or $$(-r_A) = \frac{F_{Ao}\ X_A\ [1 + (\frac{W_s}{G})\ \frac{\rho_G}{\rho_s}]}{(\frac{W_s}{G})\ \rho_G\ V} \qquad (11)$$

Equation (11) was used to calculate the reaction rate.

6.3 Kinetic Results

The rate of reaction was calculated from equation (11) as the rate of formation of o-tolualdehyde per unit time per unit weight of

catalyst. This assumes that all the o-xylene that reacts forms o-tolualdehyde.

The conversion was taken as the number of moles of o-tolualdehyde in the reactor discharge stream per mole of o-xylene in the inlet stream.

Figure 12 shows the rate of reaction as a function of the inlet o-xylene concentration plotted on logarithmic co-ordinates. For the three highest values of inlet concentration, the ordinate is the mean of all rates measured at that concentration, with the range of measured rates shown by a vertical line. At the lowest concentration (1.16×10^{-5} lb.-moles/ft.^{3}) only one rate measurement was obtained. The abscissa is the average inlet concentration of o-xylene at a particular set of reactor conditions.

Table 3 lists all the data for Figure 12. Complete measured and calculated data and the procedures employed to calculate the reaction rate and inlet concentration are listed in Appendix 1.

A best fit straight line through all the rate data was obtained by linear regression analysis and is shown on Figure 12. It is assumed that the reaction rate can be expressed by a power function rate equation:

$$(-r_A) = k_A C_A^n$$

Taking logarithms, $\ln(-r_A) = \ln k_A + n \ln C_A$.

Hence a plot of $(-r_A)$ vs. C_A on logarithmic co-ordinates will have a slope of n, the order of the reaction, and an intercept of k_A, the reaction rate constant.

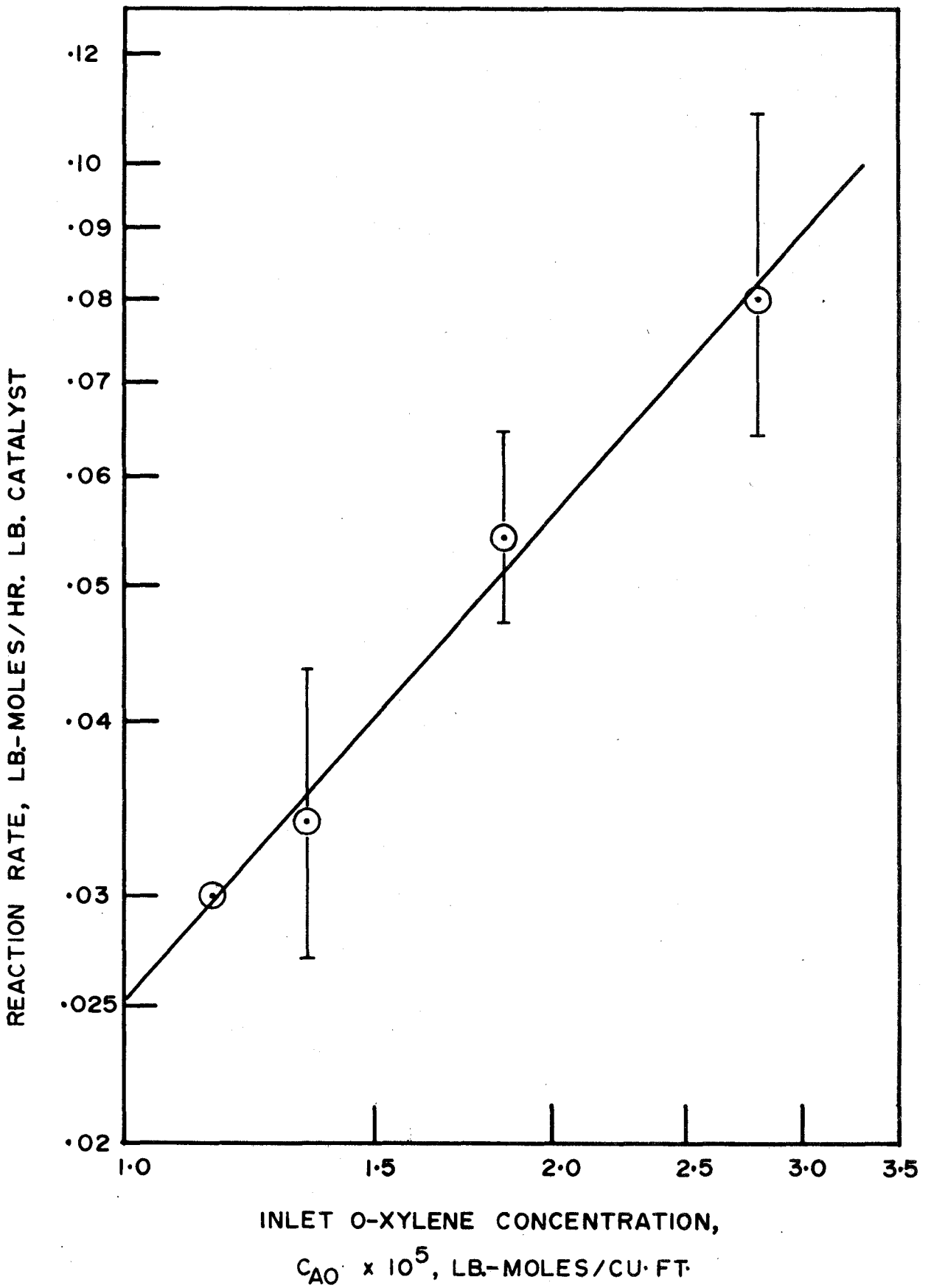
·12
·10
·09
·08
·07
·06
·05
·04
·03
·025
·02
REACTION RATE, LB.-MOLES/HR. LB. CATALYST
1·0
1·5
2·0
2·5
3·0
3·5
INLET O-XYLENE CONCENTRATION,
C_{AO} x 10^5, LB.-MOLES/CU·FT·

TABLE 3

REACTION RATE DATA

O-Xylene Feed Rate lb./hr.	Air Feed Rate lb./hr.	Inlet O-Xylene Conc.^{n} lb.-moles/ft.^{3}	Reaction Rate lb.-moles/hr. lb. cat.
0.70	19.8	1.16×10^{-5}	0.030
0.85	19.9	1.45	0.044
0.85	20.7	1.33	0.032
0.85	20.7	1.33	0.027
0.85	20.7	1.33	0.029
0.85	20.7	1.34	0.031
0.85	21.3	1.30	0.038
1.16	19.8	1.91	0.044
1.16	19.8	1.91	0.047
1.16	19.8	1.91	0.044
1.16	20.7	1.78	0.064
1.16	20.7	1.80	0.064
1.16	20.7	1.80	0.062
1.81	19.9	2.85	0.075
1.81	19.9	2.85	0.067
1.81	19.9	2.85	0.065
1.81	19.8	2.85	0.065
1.81	20.2	2.82	0.064
1.81	20.7	2.77	0.076
1.81	20.7	2.71	0.096
1.81	20.7	2.71	0.072
1.81	20.7	2.72	0.070
1.81	20.7	2.72	0.111
1.81	20.7	2.72	0.072
1.81	20.9	2.77	0.071
1.81	20.9	2.77	0.106
1.81	20.9	2.77	0.104

The regression analysis of the rate data gives:

$$n = 1.1$$

$$k_A = 10^4 \frac{\text{ft.}^3}{\text{hr. lb. catalyst}}$$

The correlation coefficient for the regression is 0.88 and is significant at the 99% level.

The reaction rates plotted on Figure 12 have been corrected for differences between the reaction temperature and the reference temperature of 750°F. The reaction temperature is the mean of the solids temperature at the bottom of the solids hold-up tank, the temperature at the bottom elbow of the reactor, and the temperature at the top elbow. This average temperature fluctuated between 730°F and 820°F during the experimental work. A correction factor, calculated by assuming an Arrhenius-type temperature dependency of the rate constant and using an activation energy of 9200 cal/mole as reported by Costa Novella and Benlloch (18), was applied to each observed reaction rate.

The measured reaction rate reported here was not, however, corrected for the contribution to the overall rate of the homogeneous, i.e., non-catalytic, reaction. As will be shown subsequently, the homogeneous rate appears to account for a negligible portion of the conversion.

7. DISCUSSION OF RESULTS

7.1 Product Distribution

The presence in the reactor discharge stream of a relatively large amount of o-tolualdehyde and minute quantities of o-toluic acid, phthalic anhydride, and phthalide, suggest that o-tolualdehyde is an intermediate in the oxidation process and that the reaction rate is not rapid enough to form significant amounts of subsequent products. This inference is supported by the fact that OTA, OTAc, phthalide, and PA represent increasing degrees of oxidation of o-xylene:

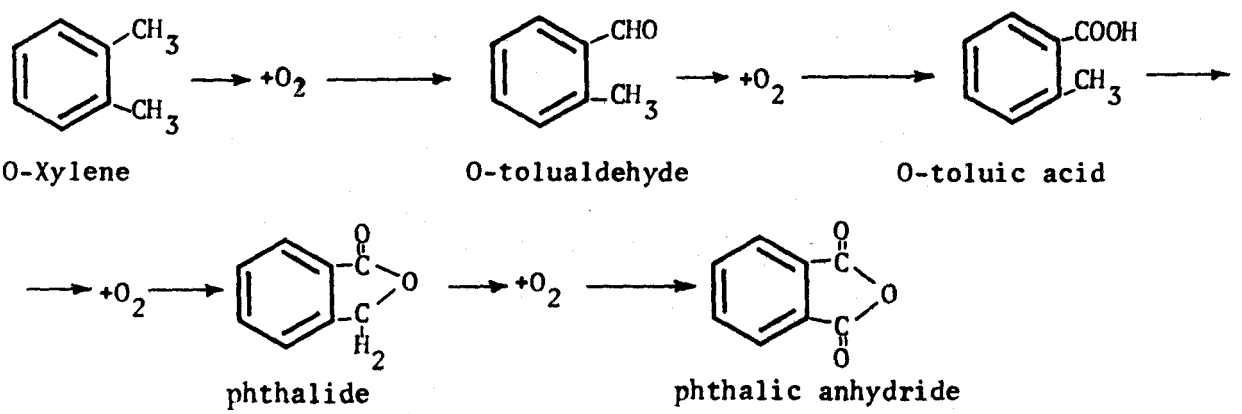

The low yields of the latter three compounds can probably be attributed to:

(a) Low concentration of catalyst

At the maximum solids-to-gas ratios employed in this study (22.8 lb./lb.) the void fraction in the reactor was 98.92%. In a conventional dense-phase fluidized bed the voidage is of the order of 70% (4).

(b) Low reaction temperature

Temperature has a strong influence on the reaction rate, the activation energy being approximately 20 kcal/mole (35). This means that at the temperature of this study (400°C) a temperature increase of 30°C would double the reaction rate. Vrbaski and Mathews (35) found that phthalic anhydride did not begin to form below a reaction temperature of about 390°C. Below 390°C o-tolualdehyde was their main product, while phthalic anhydride did not form in appreciable quantities until about 420°C.

(c) A temperature gradient in the reactor

The temperature actually dropped about 20°F from the bottom elbow to the top elbow. This was caused by heat losses from the gas-solid mixture. As previously stated, the reactor was not operated with the fused-salt circulating because of heat input limitations. The resulting temperature decrease caused the reaction rate to decrease from inlet to outlet of reactor.

(d) The short contact time

The contact time for this work was 0.2 seconds. This value was imposed by the restriction that the flow be fully turbulent. Contact times normally employed for fluidized beds range from 0.5 seconds to 2.0 seconds. (Refer to Table 1.)

Numerous discrepancies exist in the literature regarding the products formed and the reaction temperatures. Vrbaski and Mathews (35) report no phthalic anhydride below 400°C. Mann (37) reports up to 25%

yields of phthalic anhydride at temperatures from 300°C to 334°C. Costa Novella and Escardino (16, 17, 18) found that the optimum yield of phthalic anhydride was 55% and that it occurred at 310°C. Carra and Beltrame (23) observed a phthalic anhydride yield of 18% at 460°C.

Undoubtedly, the different catalysts employed by the different workers can account for some of the discrepancies. Also, some of the analytical methods may not detect all the products. However, the method of measuring the reaction temperature could have an important bearing on the observations.

Mann (37) measured the reaction temperature by inserting a thermocouple into the reactor wall. Vrbaski and Mathews (35, 36) inserted a thermowell into the catalyst bed. In both of these studies, the actual reaction temperature on the catalyst surface is uncertain. Because of the steep temperature gradients in a packed bed, it is quite possible that the reaction is occurring at a considerably higher temperature than the reported temperature.

In the reactor used for this study, heat transfer between the gas and solid is extremely rapid. This is because of the intimate gas-solid contact, the large heat transfer area available, and the turbulent flow patterns. Therefore, it is felt that the reaction temperatures reported in this study are almost identical to the true reaction temperatures.

The conclusions that can be drawn about the mechanism of the reaction from the results of this work are limited by the fact that neither the contact time nor the reaction temperature was varied and the

temperature control was poor. However, the distribution of products, i.e., a large yield of o-tolualdehyde, and small yields of o-toluic acid, phthalide, phthalic anhydride, and maleic anhydride, is consistent with the mechanisms postulated by other workers. It appears that phthalic anhydride has been formed by way of o-tolualdehyde, o-toluic acid and phthalide as intermediates and that maleic anhydride has been formed by a parallel reaction. This agrees with the mechanism proposed by Vrbaski and Mathews (35) who found that phthalic anhydride was formed by either the sequential path described above or directly. Temperatures above 420°C favoured the direct route, while the sequential route predominated below 400°C. These workers also report the formation of small amounts of maleic anhydride which formed from a parallel reaction step. The formation of o-tolualdehyde as an intermediate in the oxidation to phthalic anhydride and a parallel reaction to form maleic anhydride was proposed by Simard (21), and Costa Novella and Escardino Benlloch (16, 17, 18). These workers do not report any o-toluic acid or phthalide. However, their analytical methods were by quantitative analysis and it is quite possible that not all the reaction products were detected.

7.2 Kinetic Behaviour

The method of calculating the reaction rate in this study involves several assumptions in addition to those listed in section 6.2. A discussion of these additional assumptions follows.

(a) The reaction rate reported here is the rate of formation of o-tolualdehyde. This implies that all the o-xylene that reacts forms

o-tolualdehyde. A more correct method would have been to calculate the rate of disappearance of o-xylene. However, because of the low conversions obtained (the highest conversion being 17%), the calculation of the amount of o-xylene disappeared involves measuring small changes in large quantities. Such a procedure is prone to large errors. The conversions calculated from the amount of o-xylene disappeared were neither reproducible nor logical.

The calculation of the rate neglects any reaction products other than o-tolualdehyde. This appears to be reasonable, considering the results of other workers. Vrbaski and Mathews (35, 36), Carra and Beltrame (23), and Costa Novella and Benlloch (17) all found phthalic anhydride to be the main product with the yields of maleic anhydride, carbon oxides, and other products being considerably less. The amount of phthalic anhydride formed in this work is insignificant. Therefore the yields of other products, which would be expected to be less than the PA yield, should also be insignificant.

(b) The observed reaction rate was not corrected for the homogeneous reaction. The homogeneous reaction rate could not be measured experimentally because as soon as the solids feed was stopped, temperatures in the reactor began to climb rapidly. With no solids flowing through the reactor and no salt flow in the reactor jacket, most of the heat generated by the homogeneous reaction was absorbed by the flowing gases. Thus, even though the homogeneous reaction rate was probably small, the low heat capacity of the gas stream resulted in a temperature increase.

In the absence of experimental data, the extent of homogeneous reaction was estimated from the work of Loftus (26), who found the homogeneous reaction to be first-order with the rate constant given by:

$$\ln k = 10.05 - 20{,}000/RT$$

where k = rate constant, $sec.^{-1}$, and the activation energy is 20,000 cal./gm. mole.

Applying this equation to the conditions of this study, the maximum contribution of the homogeneous reaction, i.e., at the lowest conversion measured, is 10%. Since this is within the experimental accuracy of the rate measurements, the effect of the homogeneous reaction has been neglected.

The usefulness of comparing results from kinetic studies made with different catalysts is doubtful. This is because the mechanism of catalysis is poorly understood. Consequently, kinetic studies conducted under similar reaction conditions (contact time, temperature, feed composition) but with slightly different catalysts result in markedly different reaction rates and product distributions.

Nevertheless, Table 4 lists the reaction rate constants for the disappearance of o-xylene reported by other workers along with the value determined from this study. All values are referred to 400°C. Table 4 also tabulates the characteristics of the catalysts used in the different studies.

Despite the wide range of rate constants, two facts are apparent from Table 4:

TABLE 4

COMPARISON OF RATE CONSTANT FROM THIS WORK WITH PUBLISHED VALUES

Reference	Catalyst			Rate Constant, $Ft.^3/Hr.\ Lb.\ Cat.$
	Type	Surface Area, $M^2/Gm.$	Avg. Diam., Microns	
Mann (37)	V_2O_5:K_2SO_4 Silica Gel Support	52	1600	650
Vrbaski & Mathews (35)	Fused V_2O_5	2	N.A.	0.5
Novella & Benlloch (16, 18)	V_2O_5:K_2SO_4 Silica Gel Support	N.A.	150	40
Carra & Beltrame (23)	V_2O_5 on Earth Support	N.A.	50	0.2
This Study	V_2O_5:K_2SO_4 Silica Gel Support	171	45	10,000

N.A. = Not Available

(a) the rate constants are higher for silica-gel supported catalysts.

(b) the rate constant from this study is considerably larger than that reported by other workers using a similar catalyst.

Considering the extremely high rate constant found in this study, one could speculate that several factors are responsible:

(a) the intimate contact between gas and solid.

The TBR is not subject to gas by-passing the solids in bubbles as is the fluidized bed. In a fixed bed reactor, stagnant regions may be present which would reduce the reaction rate.

(b) the catalyst employed for this work has a large, readily accessible surface.

This is due to the small particle size (60% of the particles are smaller than 40 microns) and to the dilute concentration of catalyst particles.

The slope of the regression line of Figure 12 is approximately equal to 1, indicating that the disappearance of o-xylene in this reactor is by a first-order reaction. As with the rate constants, there is little agreement in the literature as to the dependence of the reaction rate on hydrocarbon concentration. Reaction orders of 0.5 (35, 23), 0.7 (37), and 1 (17, 12, 24, 21) for the disappearance of hydrocarbon are reported. Probably the reason for the lack of agreement is that the reaction was investigated under conditions where different resistances were rate-controlling. It is thought (1) that at low concentrations of reactant in gas-solid catalytic reactions, the adsorption of the reactant

onto the catalyst surface is rate-controlling. Adsorption of gases at low concentrations is a linear, i.e., first-order, process. As the concentration of the reactant in the gas-phase is increased, the adsorption isotherm begins to level off and the reaction rate depends less on reactant concentration. Eventually the catalyst surface becomes saturated with reactant and the rate is independent of the gas-phase concentation, i.e., the reaction is zero-order.

7.3 Rate-Controlling Step in the Reaction

The reaction on the solid surface must proceed by the following sequence:

(a) Diffusion of reactants from the main body of fluid to the exterior surface of the catalyst.

(b) Diffusion of reactants into the pores of the catalyst particle.

(c) Chemical reaction on the catalyst surface.

(d) Diffusion of products from the catalyst pores.

(e) Diffusion of products into the main body of fluid.

The importance of each step to this investigation will be discussed.

Steps (a) & (e): Calculations, detailed in Appendix 3.2, show that for the conditions of this study, the resistance to external diffusion is negligible. This means that the concentration of o-xylene on the catalyst surface is essentially identical to its concentration in the main stream.

Steps (b) & (d): Mann (37) showed that the effectiveness factor, defined as the ratio of the reaction rate considering pore diffusion resistance to the reaction rate if all the catalyst surface were equally accessible, was equal to unity for his catalyst. Hence he neglected pore diffusion resistance in his study. Mann's average particle diameter was 1600 microns compared to 45 microns for this work. One would expect that reducing the particle size would reduce the resistance to pore diffusion; therefore, it is neglected in this investigation.

Step (c): Since internal and external resistances are assumed negligible, the surface phenomena must control the reaction rate. The surface reaction involves adsorption of o-xylene onto the catalyst surface, reaction between adsorbed o-xylene and oxygen of the catalyst, desorption of products, and regeneration of the catalyst with oxygen from the main stream. The fact that the observed reaction rate depends strongly on the concentration of o-xylene indicates that the adsorption of o-xylene is rate-controlling. If either the surface reaction, the desorption of products, or the regeneration step were rate-controlling, then the catalyst surface would always be saturated with o-xylene and the rate would be expected to be independent of o-xylene concentration.

7.4 Error Discussion

7.4.1 Reproducibility of Data

The vertical lines on Figure 12 indicate that the measured reaction rates vary considerably about the mean. This variation ranges from $\pm$ 20% to $\pm$ 40%. Another indication of the variation of rates can be

obtained from the linear regression analysis. The standard error of the estimate, which is a measure of the variance in the rate left unexplained by the inlet o-xylene concentration, is .0122. This is approximately 20% of the average reaction rate.

7.4.2 Sources of Error

The variation in reaction rate values at a particular value of inlet o-xylene concentration is caused by two effects: errors in the measurement of variables required to calculate the reaction rate, and variations of the phenomenon itself.

The maximum variation in the rate that could be expected from measurement errors is $\pm$ 20%. This was calculated by considering the relative error of each variable of equation (11). Appendix 3.4 gives the details of this calculation.

Because an instantaneous sampling method was used for obtaining the kinetic data, it is quite conceivable that the maximum variation in rate due to measurement errors could occur. All the kinetic studies reported in the literature utilize an analysis method in which the reaction products are collected during a measured period of time -- usually several minutes. At the end of this period, samples taken from the collected condensate are analyzed. Such a procedure would tend to "average" or damp out fluctuations in the variables which occurred during the collection period. The sampling method of this study has no averaging effect, the sample being representative of an extremely short reaction period, i.e., the time necessary to change the contents of

the sample loop.

The actual variation in reaction rates is larger than can be expected from the error analysis. This implies that phenomonological processes are taking place which are not accounted for by the method of analyzing the data. The nature of these processes is open to conjecture at this stage.

In the following paragraphs, what are considered to be the most plausible explanations for the variation in reaction rate beyond what can be expected from experimental error are discussed.

(a) Unsteady-state temperature conditions prevail in the reactor. The temperature of the gas mixture entering the reactor differed by as much as 200°F from the temperature of the solids raining into the discharge cone. Hence the initial stages of the reaction occurred in an unsteady-state region. In fact, as mentioned previously, the reaction temperature dropped throughout the entire length of the reactor. The effect of these transient temperatures is difficult to predict. As a first approximation, an average reaction temperature has been calculated and a correction factor relating this average temperature to a reference temperature has been applied to the measured reaction rate. In fact, the effect of temperature on the rate should be integrated along the reactor. This necessitates a detailed knowledge of the variation of temperature throughout the reactor. This information was not available.

The reaction rate-concentration curve depends to some extent on

which temperature is called the reaction temperature. For the data plotted on Figure 12, the reaction temperature is the mean of the temperature of the solids entering the feeder, the temperature at the bottom elbow and the temperature at the top elbow. A linear regression analysis was performed on the same data but taking as the temperature the temperature at the bottom elbow. The resulting regression line has a similar slope and intercept to the line on Figure 12 but the data are more scattered. The correlation coefficient for the single temperature regression is 0.82 compared to 0.88 for Figure 12.

(b) Mixing may be occurring in the reactor. The analysis of the data assumes plug flow of both the gas and the solids. If longitudinal mixing of either phase is taking place, there will be a distribution of residence times and the rate will be different from that calculated from the plug flow model. In a recent paper, Bischoff and McCracken (53) raise the question that data scatter in the correlation of two-phase flow operations may be caused by the complete neglect of the mixing variable by the plug flow model.

Related to the residence time of gas and solids in the reactor is the small amount of gas that by-passes the reactor and flows through the solids hold-up tank. In effect, this gas flows through a packed-bed reactor. The residence time of the gas in the hold-up tank would be many times longer than the residence time in the reactor. Therefore, although the gas flow through the tank is small, it may have a significant effect on both the product distribution and kinetic behaviour.

7.5 Observed Effects

7.5.1 Colour Change of Catalyst

During the course of the reaction, the catalyst underwent a change in colour from olive green to a brownish orange. When a sample of used catalyst was oven-dried prior to surface area measurement, it reverted to its original olive green colour.

These observations indicate that the catalyst had been reduced somewhat by the reaction and that it was reoxidized while in the oven. This is in accordance with the literature (21, 35, 16, 17, 18, 19) in which it is proposed that the oxygen for the oxidation is supplied by the catalyst.

The reduction of the catalyst did not appear sufficient to affect its activity. For a given inlet o-xylene concentration, the reaction rate was approximately the same at the beginning and end of the run. Over a longer reaction period (the longest reaction period in this study was twenty hours) the activity of the catalyst could possibly undergo a significant decrease. This should be investigated in future work.

8. CONCLUSIONS AND RECOMMENDATIONS

8.1 Conclusions

(a) The gas-phase catalytic oxidation of o-xylene can be conducted in a transported-bed reactor in which the catalyst is present in dilute concentrations.

(b) The reaction products observed in this work are consistent with the reaction mechanisms proposed by other workers. O-tolualdehyde was the principal product of the reaction, with small amounts of maleic anhydride, o-toluic acid, phthalide, and phthalic anhydride also being formed.

(c) The rate of reaction was found to be proportional to the inlet concentration of o-xylene for the conditions of this study. A first-order process suggests that the adsorption of o-xylene on the catalyst surface is the rate-controlling step of the reaction.

(d) An extremely large rate constant was observed in this investigation, relative to that found by other workers. It is submitted that the large rate constant can be attributed to the intimate gas-solid contact obtained in this reactor and to the large, readily accessible surface of the catalyst employed.

8.2 Recommendations

It is recommended that further work with this reactor should consist of the following:

(a) Investigation of the effect of temperature on the reaction - This would require first that the temperature be controlled closely, i.e.,

provision must be made for more heat input to the salt circulation system so that the reaction temperature could be made uniform and equal to the temperature of the salt flowing through the reactor jacket.

(b) The effect of higher solids loading should be studied. The solids-to-gas ratio in this study was limited not by the maximum amount of solids the gas stream could transport, but by the maximum speed of the variable speed solids feeder drive.

(c) The extent of the non-catalytic reaction should be measured experimentally. This would be possible once recommendation (a) is implemented.

(d) Studies should be made of the residence time distribution in the reactor. Knowledge of the residence time distribution would allow the development of a more realistic model than the plug flow model to describe the reaction.

9. BIBLIOGRAPHY

1. Levenspiel, O., "Chemical Reaction Engineering", Wiley, New York (1962).
2. Spielman, M., A.I.Ch.E. Journal, 10, 496 - 501 (1964).
3. Hughes, M. F., (to Calif. Res. Corp.), U.S. Patent 3,129,230 (April 14, 1964).
4. Zenz, F. A., & D. F. Othmer, "Fluidization and Fluid-Particle Systems", Reinhold, New York (1960).
5. Davidson, J. F., & D. Harrison, "Fluidized Particles", Cambridge University Press (1963).
6. Marsheck, R. M., & A. Gomezplata, A.I.Ch.E. Journal, 11, 167 - 173 (1965).
7. Murkherjee, S. P. & L. K. Doraiswamy, Brit. Chem. Eng., 10, 93 - 102 (1965).
8. Levine, I. E., "The Chemistry of Petroleum Hydrocarbons", Vol. 3, 1 - 7, Reinhold, New York (1955).
9. Klar, R., Australian Patent 167,576 (April 30, 1956).
10. Gulati, I. B., & S. K. Bhattacharyya, J. Sci. Industr. Res., India, 12B, 450 (1953).
11. Gulati, I. B., & S. K. Bhattacharyya, Chem. and Ind. (London), 1425 (1954).
12. Gulati, I. B., & S. K. Bhattacharyya, Ind. Eng. Chem., 50, 1719 - 1726 (1958).
13. Bhattacharyya, S. K., & R. Krishnamurthy, Current Science (India), 28, 363 - 364 (1959).

14. Bhattacharyya, S. K., & N. D. Ganguly, Jour. Indian Chem. Soc., 38, 463 - 480 (1961).

15. Bhattacharyya, S. K., & R. Krishnamurthy, J. Appl. Chem., 13, 547 - 552 (1963).

16. Costa Novella, E., & A. Escardino Benlloch, Anales De Fisica Y Quimica, 58B, 783 - 790 (1962).

17. Costa Novella, E., & A. Escardino Benlloch, ibid., 58B, 791 - 802 (1962).

18. Costa Novella, E., & A. Escardino Benlloch, ibid., 59B, 669 - 680 (1963).

19. Simard, G. L., et. al., Ind. Eng. Chem., 47, 1424 - 1430 (1955).

20. Levine, I. E., (to Calif. Res. Corp.), U.S. Patent 2,438,369 (March 23, 1948).

21. Emmett, P. H., Ed., "Catalysis", Vol. VII, 212 - 217, Reinhold, New York (1960).

22. Parks, W. G., & C. E. Allard, Ind. Eng. Chem., 31, 1162 - 1167 (1939).

23. Carra, S., & P. Beltrame, Chem. Ind. (Milan), 40, 1152 - 1157 (1964).

24. Satterfield, C. N., & J. Loftus, A.I.Ch.E. Journal, 11, 1103 - 1108 (1965).

25. Satterfield, C. N., & J. Loftus, I & EC Proc. Des. & Dev., 4, 102 - 105 (1965).

26. Satterfield, C. N., & J. Loftus, Jour. Phys. Chem., 69, 909 - 918 (1965).

27. Loftus, J., Sc.D. thesis, Mass. Inst. Tech. (1963).

28. Fenske, M. R., & J. H. Jones, (to Esso Res. and Eng. Co.), U.S. Patent 3,086,852 (April 23, 1963).

29. Sherwood, P. W., Oil in Canada, 24, 21212 - 21215 (1958).

30. Sherwood, P. W., ibid., 26, 21434 - 21437 (1958).

31. Sherwood, P. W., ibid., 26, 21586 - 21588 (1958).

32. Guccione, E., Chem. Eng., 132 - 134 (June 7, 1965).

33. Wright, F. J., J. Phys. Chem., 64, 1944 - 1949 (1960).

34. Wright, F. J., ibid., 66, 2023 - 2028 (1962).

35. Vrbaski, T., & W. K. Mathews, J. Phys. Chem., 69, 457 - 466 (1965).

36. Vrbaski, T., & W. K. Mathews, J. Catalysis, 5, 125 - 134 (1966).

37. Mann, R. F., Ph.D. thesis, Queen's University (1966).*

38. Lewis, W. K., and E. R. Gilliland (to Standard Oil Development Co.), U.S. Patent 2,498,088 (Feb. 21, 1950).

39. Bernardina, F., et. al., Chem. Ind. (Milan), 47, 485 - 489 (1965).

40. Longwell, J. P. (to Stand. Oil Dev. Co.), U.S. Patent 2,491,500 (Dec. 20, 1949).

41. Morrell, C. E., & L. K. Beach (to Stand. Oil Dev. Co.), U.S. Patent 2,443,832 (June 22, 1948).

42. American Cyanamid Co., Brit. Patent 731,370 (June 8, 1955).

43. Robinson, J. (to ICI), Brit. Patent 705,615 (March 17, 1954).

44. Goodson, L. B., and J. A. Guyer (to Phillips Petroleum Co.), U.S. Patent 2,606,097 (August 5, 1952).

45. Kirkbride, C. G., and J. C. Dart (to Houdry Process Corporation), U.S. Patent 2,628,188 (July 21, 1949).

---

* Kingston, Ontario, Canada.

46. Kuhn, G. F. (to Sinclair Refining Co.), U.S. Patent 2,539,583 (Jan. 30, 1951).

47. Jewell, J. W., and W. B. Johnson (to M. W. Kellogg Co.), U.S. Patent 2,543,974 (Mar. 6, 1951).

48. Bücher, H., and H. Luckow, British Patent 716,273 (Sept. 29, 1954).

49. Anonymous, Atomics, Barrington, Ill., Technical Pub. Co., 1958.

50. Kolyzhenkov, P. A., et. al., U.S.S.R. Patent 68,068 (Mar. 31, 1947).

51. Dernedde, E., M.Eng. thesis, McMaster Univ. (1966).

52. Stairmand, C. J., Trans. Instn. Chem. Engrs., 29, 356 - 383 (1951).

53. Bischoff, K. B., and E. A. McCracken, Ind. Eng. Chem., 58, 18 - 31 (1966).

54. Perry, J. H., "Chemical Engineer's Handbook", 3rd Edition, McGraw-Hill, New York (1950).

55. Braunauer, S., et. al., J. Am. Chem. Soc., 60, 309 (1938).

56. Ross, S., and J. P. Olivier, "On Physical Adsorption", 12, 66 - 67, Interscience Publishers, New York (1964).

APPENDIX 1

EXPERIMENTAL DATA

1.1 Sample Calculations

As an example of the calculation procedure, consider the first data point for which

$$C_{Ao} = 1.16 \times 10^{-5} \frac{\text{lb.-moles}}{\text{ft.}^3} \quad \text{and} \quad (-r_A) = 0.029 \frac{\text{lb.-moles}}{\text{hr. lb. catalyst}}$$

For this point, the experimental measurements were as follows:

Temperature of Solids before entering feeder, $t_1 = 807°F$

Temperature at bottom elbow, $t_2 = 818°F$

Temperature at top elbow, $t_3 = 780°F$

Feedrate of O-xylene, $F_{Ao} = 6.60 \times 10^{-3} \frac{\text{lb. moles}}{\text{hr.}}$

Feedrate of air (main plus auxiliary) = 17.9 lb./hr.

Solids feeder speed = 36 rpm

Gas sampling valve temperature, $t_4 = 251°F$

Aspirator pressure = 12 in. water

O-tolualdehyde peak area = 29.6 vernier units

From these data:

(a) Reaction Temperature, $\bar{t} = \frac{t_1 + t_2 + t_3}{3} = 801°F = 702°K$

(b) Temperature Correction Factor, $k/k_r = e^{-\frac{E}{RT} + \frac{E}{RT_r}}$

where T = reaction temperature, °K

R = 2 cal./gm.-mole °K

E = Activation energy = 9200 cal./gm.-mole

T_r = Reference temperature = 673°K (750°F)

$$k/k_r = e^{-\frac{9200}{2x702} + \frac{9200}{2x673}} = 1.31$$

(c) Gm.-moles OTA in sample = Peak area x calibration factor

$$\text{Gm.-moles OTA} = 29.6 \text{ v.u.} \times 0.131 \times 10^{-8} \frac{\text{gm.-moles}}{\text{v.u.}} = 3.89 \times 10^{-8}$$

(d) $$\text{Sample wt., gm.} = \frac{PVM}{RT}$$

where P = pressure in sample loop, atm.

= atmospheric pressure − aspirator pressure

V = volume of sample loop = 1.0 cc.

M = average molecular weight of sample = 30 gm./gm.-mole

T = sample temperature, °K

$$\text{Sample wt.} = \frac{0.985 \times 1.0 \times 30}{82.06 \times 395} = 9.13 \times 10^{-4} \text{ gm.}$$

(e) $$\frac{\text{gm.-moles OTA}}{\text{gm. sample}} = 0.426 \times 10^{-4}$$

(f) Total gas feedrate, $G = 17.9 \text{ lb./hr.} + 6.60 \times 10^{-3} \times 106 \frac{\text{lb. } O_X}{\text{lb.-mole}}$

$$= 18.6 \text{ lb./hr.}$$

(g) $$\frac{\text{lb.-mole } O_X}{\text{lb. feed}} = \frac{6.60 \times 10^{-3}}{18.6} = 3.55 \times 10^{-4}$$

(h) $$\text{Uncorrected conversion} = \frac{\text{gm.-moles OTA}}{\text{gm. sample}} \div \frac{\text{lb.-mole } O_X}{\text{lb. feed}}$$

$$= \frac{0.426 \times 10^{-4}}{3.55 \times 10^{-4}} = 0.120$$

(i) $$\text{Corrected conversion, } X_A = \frac{\text{Uncorrected conversion}}{\text{Temp. correction factor}} = 0.092$$

(j) Volumetric feedrate, $v_o = \frac{G}{\rho_G}$

where ρ_G = gas density @ average of t_2 and t_3

$$= \frac{PM}{RT} = \frac{1 \times 30}{.730 \times 1260} = 0.0326 \text{ lb./ft.}^3$$

$$v_o = \frac{18.6}{.0326} = 570 \text{ ft.}^3\text{/hr.}$$

(k) Inlet concentration of o-xylene, $C_{Ao} = \frac{F_{Ao}}{v_o} = 1.16 \times 10^{-5} \frac{\text{lb.-moles}}{\text{ft.}^3}$

(l) Solids feedrate, W_s lb./hr. = rotor rpm x $\frac{\text{volume}}{\text{revolution}}$ x bulk density x 60

$$36 \times 0.00404 \frac{\text{ft.}^3}{\text{rev.}} \times 39 \frac{\text{lb.}}{\text{ft.}^3} \times 60 = 340$$

(m) $W_s/G = 340/18.6 = 18.3$

(n) $(-r_A)$ from equation (11) = $\frac{F_{Ao} X_A \left[1 + \left(\frac{W_s}{G}\right) \frac{\rho_G}{\rho_s}\right]}{\left(\frac{W_s}{G}\right) \rho_G V}$

where ρ_s = true density of catalyst, = 131 lb./ft.^{3}

V = volume of reactor, = 0.0346 ft.^{3}

$$(-r_A) = \frac{(6.6 \times 10^{-3}) (0.092)}{(18.3) (0.0326) (0.0346)} = 0.029 \frac{\text{lb.-moles}}{\text{hr. lb. catalyst}}$$

1.2 Listing of Data

This section lists the measured data and the experimental data calculated by the procedure described in the preceeding section. Column headings are defined on the following page.

Column Number	Definition
1	t_1, °F
2	t_2, °F
3	t_3, °F
4	$\bar{t}$, °F
5	t_4, °F
6	temperature correction factor, k/k_r
7	$F_{Ao} \times 10^3$, lb. moles/hr.
8	G, lb./hr.
9	W_s, lb./hr.
10	W_s/G
11	lb.-mole OX/lb. feed $\times 10^4$
12	gm-mole OTA $\times 10^8$
13	sample wt. $\times 10^4$, gm.
14	gm.-mole OTA/gm. sample $\times 10^4$
15	uncorrected conversion
16	X_A, corrected conversion
17	ρ_G, lb./ft.^{3}
18	v_o, ft.^{3}/hr.
19	$C_{Ao} \times 10^5$, lb. moles/ft.^{3}
20	$(-r_A)$, lb.-moles/hr. lb. catalyst

TABLE 5

EXPERIMENTAL DATA

(1)	(2)	(3)	(4)	(5)	(6)	(7)	(8)	(9)	(10)
807	818	780	801	251	1.310	6.60	18.6	340	18.3
742	742	712	732	289	0.904	8.02	20.8	355	17.1
765	917	776	819	284	1.433	8.02	21.6	492	22.8
773	795	769	778	284	1.162	8.02	21.6	492	22.8
773	791	769	777	284	1.162	8.02	21.6	492	22.8
773	791	765	776	284	1.150	8.02	21.6	492	22.8
771	799	761	776	284	1.150	8.02	22.2	492	22.1
764	803	745	770	291	1.116	11.00	21.0	439	20.8
762	784	745	763	291	1.083	11.00	21.0	439	20.8
758	784	745	762	291	1.072	11.00	21.0	439	20.8
789	818	780	795	284	1.271	11.00	21.9	492	22.4
788	799	776	787	284	1.221	11.00	21.9	492	22.4
787	795	773	784	284	1.209	11.00	21.9	492	22.4
752	746	720	739	290	0.932	17.10	21.7	355	16.4
745	754	723	740	291	0.942	17.10	21.7	355	16.4
752	788	731	756	291	1.020	17.10	21.7	355	16.4
755	806	739	766	291	1.083	17.10	21.7	355	16.4
823	810	773	801	262	1.310	17.10	21.6	340	15.7
820	810	773	800	269	1.310	17.10	22.0	340	15.4
800	806	780	795	280	1.271	17.10	22.5	492	21.9
799	806	780	794	280	1.258	17.10	22.5	492	21.9
796	799	780	792	277	1.258	17.10	22.5	492	21.9
796	799	780	792	284	1.258	17.10	22.5	492	21.9
796	795	776	788	284	1.258	17.10	22.5	492	21.9
791	776	731	765	284	1.083	17.10	22.7	186	8.2
792	776	727	764	284	1.083	17.10	22.7	186	8.2
793	776	731	766	284	1.083	17.10	22.7	186	8.2

TABLE 5 (continued)

(11)	(12)	(13)	(14)	(15)	(16)	(17)	(18)	(19)	(20)
3.55	3.89	9.13	0.426	0.120	0.092	0.0326	570	1.16	0.029
3.86	3.82	8.69	0.439	0.111	0.123	0.0376	552	1.45	0.044
3.71	5.68	8.69	0.653	0.176	0.123	0.0360	602	1.33	0.032
3.71	3.46	8.69	0.398	0.107	0.092	0.0360	602	1.33	0.027
3.71	3.85	8.69	0.443	0.120	0.103	0.0360	602	1.33	0.029
3.71	4.92	8.69	0.567	0.153	0.133	0.0361	599	1.34	0.031
3.61	4.70	8.69	0.541	0.150	0.130	0.0360	617	1.30	0.038
5.23	5.48	8.63	0.636	0.121	0.105	0.0365	576	1.91	0.044
5.23	5.55	8.63	0.643	0.123	0.114	0.0365	576	1.91	0.047
5.23	5.09	8.63	0.591	0.113	0.105	0.0365	576	1.91	0.044
5.02	9.01	8.69	1.038	0.206	0.162	0.0356	616	1.78	0.064
5.02	8.62	8.69	0.992	0.198	0.162	0.0358	612	1.80	0.064
5.02	8.22	8.69	0.947	0.188	0.156	0.0359	610	1.80	0.062
7.88	5.65	8.67	0.652	0.083	0.089	0.0362	600	2.85	0.075
7.88	5.22	8.65	0.603	0.077	0.082	0.0362	600	2.85	0.067
7.88	5.48	8.65	0.633	0.080	0.079	0.0362	600	2.85	0.065
7.88	5.74	8.65	0.633	0.084	0.077	0.0362	600	2.85	0.065
7.92	6.79	9.02	0.753	0.095	0.073	0.0357	605	2.82	0.064
7.78	7.64	8.86	0.862	0.111	0.085	0.0357	617	2.77	0.076
7.60	12.73	8.73	1.460	0.192	0.151	0.0356	632	2.71	0.096
7.60	9.46	8.73	1.082	0.142	0.113	0.0356	632	2.71	0.072
7.60	9.33	8.78	1.062	0.140	0.111	0.0358	628	2.72	0.070
7.60	14.62	8.67	1.688	0.222	0.176	0.0358	628	2.72	0.111
7.60	9.46	8.67	1.091	0.143	0.116	0.0359	628	2.72	0.072
7.53	3.00	8.69	0.345	0.046	0.043	0.0368	617	2.77	0.071
7.53	4.50	8.69	0.518	0.069	0.064	0.0368	617	2.77	0.106
7.53	4.44	8.69	0.512	0.068	0.063	0.0368	617	2.77	0.104

APPENDIX 2

GAS CHROMATOGRAPHIC ANALYSIS

2.1 Choice of Column

The selection of the column (25% silicone oil plus 2% phosphoric acid on Chromosorb W 60/80 mesh) for this work followed a considerable amount of experimentation with different columns.

A wide range of boiling points of the components of interest presented the major analytical problem. At a column temperature high enough to elute the least volatile component (phthalic anhydride) in a reasonable time, the most volatile component (o-xylene) was eluted extremely rapidly. A chromatograph equipped with temperature programming, in which the column temperature could be increased systematically during the elution of a sample, would have simplified the analysis immensely. However, such an instrument was unavailable.

A second analytical problem was the tendency of maleic anhydride and o-xylene to be eluted at the same time. If the carrier gas flowrate and/or column temperature was reduced in an effort to separate MA and OX, the retention time of the less volatile compounds became unreasonably long.

A brief history of the column evaluation work is presented in the following table. The table includes the partitioning agent, the column packing, column temperature, carrier gas flowrate, and comments on the performance.

TABLE 6

CHROMATOGRAPHIC COLUMN EVALUATION

Col. No.	Column		Col. Temp °C	C.G. Flow cc./min.	Comments
	Partitioning Medium	Support			
1	20% silicone oil + 2% H_3PO_4	Chromosorb W 60/80 Mesh	150	80	Peaks for all components individually. In a mixture, OX and MA eluted at the same time.
2	10% silicone oil	Chromosorb T (Teflon) 40/60 Mesh	160	92	Peaks for all components in a mixture. Separated OX and MA. Elution extremely slow (5 hours for PA).
3	20% ethylene glycol phthalate	Chromosorb W 60/80 Mesh	195	133	Elution extremely slow. At 30 minutes, still no peaks for MA, OTA, or PA.
4	20% silicone oil + small amounts of a 50-50 mixture of Bentone 34 and diisodecylphthalate	Chromosorb W 60/80 Mesh	180	80	Separated all peaks in a mixture but elution too slow (about 30 minutes for PA)
5	25% silicone oil + 2% H_3PO_4	Chromosorb W 60/80 Mesh	250	106	Best column of those tried. Separated all components of a mixture in a reasonable time (about 10 minutes for PA).

Column 5, while the best of those tried, still had several deficiencies. OTA and PA peaks tailed more than is desirable. Also, at the high column temperature necessary to achieve a reasonable analysis time, some evaporation of the partitioning medium occurred. Over a period of three weeks of operation, retention times decreased by 20%.

Retention times of the components with column 5 under the conditions of this study are given by Table 7.

TABLE 7

CHROMATOGRAPHIC COLUMN RETENTION TIMES

Compound	Retention Time to Max. Peak Ht, sec.
O-Xylene	49
Maleic Anhydride	75
O-Tolualdehyde	110
Phthalic Anhydride	540

2.2 Calibration

Column 5 was calibrated as follows:

(a) Solutions of 0.5, 1.0, and 2.0 wt. % of each of OX, MA, OTA, and PA in acetone (twelve solutions in all) were accurately prepared.

(b) A 1, 2, and 3 microliter sample of each solution was injected into the chromatograph with a 10 microliter Hamilton syringe and analyzed. Three injections of each solution were made in order to insure reproducibility. This gave twenty-seven pairs of recorder

response -- gm.-mole points for each component.

(c) A straight line was fitted to the recorder response -- gm.-mole points for each compound by linear regression analysis. The slope of this line gives the relationship between sample size and recorder response. For OX, MA, and PA, the recorder response measured was peak height, while peak areas were measured for OTA. The results of the linear regression analyses were:

OX: Gm.-moles = (0.99×10^{-8}) (Peak Height, %)

MA: Gm.-moles = (0.14×10^{-8}) (Peak Height, %)

OTA: Gm.-moles = (0.13×10^{-8}) (Peak Area, Vu)

PA: Gm.-moles = (0.92×10^{-8}) (Peak Height, %)

In order to check the calibration method, known mixtures of air and o-xylene were fed to the reactor at conditions (low temperature, no catalyst) under which no reaction took place. Gas samples from the sample point at the top of the cyclone were analyzed and the amount of o-xylene in the sample calculated from the o-xylene calibration curve. This value should agree with the amount of o-xylene in the feed which is known from the air and o-xylene rotameter calibrations.

A considerable difference existed between the two values. The amount of o-xylene per unit weight of feed (from rotameter calibrations) was from 27% to 22% lower than the amount of o-xylene per unit weight of sample (from chromatograph calibrations). It is felt that this difference can be explained by the following line of reasoning. When liquid samples are injected into a chromatograph, a finite time is required to

vapourize the sample. Therefore, it would be expected that the peak for a liquid would not be as high as the peak for a gas sample of the same volume, although the area should be equal, i.e., the gas sample peak would be sharper. In this work liquid samples were used for calibration but gas samples were taken from the reactor. Hence, the calibration would predict more o-xylene than was actually present in the sample. Furthermore, this effect should be more pronounced for larger samples. This was observed: the difference noted above was greatest at the smallest air:o-xylene ratios.

The conversions reported in this thesis should not be affected by the phenomenon described above because the conversion was calculated from the amount of OTA formed. The gm.-moles of OTA in the sample was determined from its peak area. Peak area should be identical for liquid or gas samples.

2.3 Future Improvements in Analytical Method

The analytical method could be improved by the following additions and changes:

(a) Use of a temperature-programmed chromatograph.
This would increase the separation of the more volatile compounds while decreasing the overall analysis time per sample.

(b) Addition of columns (silica gel and molecular sieve) to detect CO_2 & CO.

(c) Calibration under conditions matching as closely as possible the analysis conditions.

This would mean calibrating with gas samples of approximately the same composition as the reactor discharge stream.

Steps (b) and (c) would enable all the components of the discharge stream to be analyzed accurately and a material balance to be made.

APPENDIX 3

CALCULATIONS

3.1 Maximum Temperature Attainable if Complete Combustion Occurs

One of the principal advantages of the Transported-Bed Reactor is the uniform temperature throughout the reactor. Even if complete combustion occurs, temperatures will remain at safe levels. To illustrate, consider the worst possible case, i.e., the maximum o-xylene flowrate and the minimum solids loading. Assume that all the o-xylene is converted to CO_2 and water, and that the reactor is adiabatic. For this condition:

$F_{Ao} = 17.1 \times 10^{-3}$ lb.-moles/hr.

$G = 22.5$ lb./hr.

$W_s = 186$ lb./hr.

A steady-state heat balance on the reactor gives,

$$W_s C_{Ps} (t - 750) + G C_{PG} (t - 750) = \Delta Hr F_{Ao}$$

where: t = maximum temperature reached by gas-solids mixture

C_{Ps} = specific heat of solids, BTU/lb. °F

= 0.32 (ref. 54 for silica)

C_{PG} = specific heat of gas, BTU/lb. °F

= 0.25 (taken as air)

ΔHr = heat of reaction for complete combustion

$= 1.06 \times 10^{6}$ BTU/lb.-mole OX (ref. 8)

Solving the heat balance equation,

$t = 1030°F$

3.2 External Diffusion Resistance

In a gas-solid catalytic reaction, it is important to know the magnitude of the resistance to diffusion of the gas from the main stream to the catalyst surface. If this resistance is large enough it may control the overall rate of reaction. The approach generally taken is to calculate the concentration difference, or driving force, necessary to transfer reactant through the gas film at a rate equal to the observed reaction rate. If the concentration difference is insignificant compared to the concentration in the main stream, then the diffusion resistance is negligible.

In a TBR, diffusion by convection is difficult to estimate because the velocity of the solids relative to the gas is not known. Therefore, the worst case has been assumed, i.e., all diffusion is by a molecular mechanism. For this limiting case, the Sherwood number approaches two (ref. 54, p. 546).

That is $$N_{SH} = 2 = \frac{k_G \, RT \, d_p}{D} \qquad (1)$$

where N_{SH} = Sherwood Number

k_G = Mass transfer coefficient, $\frac{\text{gm.-moles}}{\text{sec. cm.}^2 \text{ atm.}}$

d_p = particle diameter, cm.

D = molecular diffusion coefficient of the diffusing species, $\text{cm.}^2/\text{sec.}$

R = 82.06 atm. $\text{cm.}^3/\text{gm.-mole, } ^\circ\text{K}$

T = 750°F = 673°K

The concentration difference will be calculated for the largest particle size as it will offer the largest resistance to diffusion.

d_p for largest particles = 140 microns = 0.0140 cm.

For o-xylene diffusing in air, D = 0.240 $cm.^2/sec.$ (taken from Mann's thesis (37)).

Solving equation (1) for k_G,

$$k_G = \frac{2 \times 0.240}{82.06 \times 673 \times 0.0140} = 6.2 \times 10^{-4}$$

The molar flux, N, of o-xylene can be calculated from the reaction rate and the specific surface of the particle:

Maximum reaction rate observed = 0.111 lb.-moles/hr. lb. catalyst

$$= 3.08 \times 10^{-5} \text{ gm.-moles/sec. gm. catalyst}$$

specific surface of particles $= \frac{6}{d_p \rho_s} = \frac{6}{0.0140 \times 2.1} = 204 \text{ cm.}^2/\text{gm.}$ (not considering interior pore surface)

Then $$N = \frac{3.08 \times 10^{-5} \text{ gm.-moles/sec. gm. catalyst}}{204 \text{ cm.}^2/\text{gm. catalyst}}$$

$$= 1.51 \times 10^{-7} \text{ gm.-moles/sec. cm.}^2$$

From Fick's Law, $N = k_G (C_{AB} - C_{AS})$

where C_{AB} = Concentration of o-xylene in the main stream, atm.

C_{AS} = Concentration of o-xylene on the catalyst surface, atm.

$$C_{AB} - C_{AS} = \frac{1.51 \times 10^{-7}}{6.2 \times 10^{-4}} = 2.44 \times 10^{-4} \text{ atm.}$$

Minimum mainstream concentration = $1.16 \times 10^{-5} \frac{\text{lb.-moles}}{\text{ft.}^3} = 1.02 \times 10^{-2}$ atm.

It is seen that under the most conservative conditions, the concentration difference required to transfer the reactant to the catalyst surface is only 2% of the mainstream concentration. Therefore, the concentration on the catalyst surface can be considered equal to the mainstream concentration and external diffusion resistance can be neglected.

3.3 Estimation of Homogeneous Reaction Rate

The estimate of the contribution of the homogeneous reaction is based on the first-order rate constant reported by Loftus (26).

$$\ln k = 10.05 - 20{,}000/RT$$

For $T = 750°F = 673°K$,

$$k = 0.021 \text{ sec.}^{-1}$$

A material balance for a plug flow reactor, assuming a first-order reaction, gives

$$k \frac{V}{v_o} = \ln \frac{1}{1 - x_A}$$

where V = reactor volume, ft.^3

v_o = volumetric feedrate, $\text{ft.}^3/\text{hr.}$

x_A = conversion due to homogeneous reaction

For this study, $\frac{V}{v_o}$ was essentially constant at 0.2 seconds.

Then, from the material balance equation, $X_A = 0.0042$.

The smallest conversion measured during the catalytic reaction was 0.043.

Therefore, the homogeneous reaction would be expected to contribute less than 10% to the measured conversion of the catalytic reaction.

3.4 Relative Error in Measurement of Reaction Rate

The reaction rate is calculated from equation (11):

$$(-r_A) = \frac{F_{Ao}\, X_A \left(1 + \left(\frac{W_s}{G}\right) \frac{\rho_G}{\rho_s}\right)}{\left(\frac{W_s}{G}\right) \rho_G\, V}$$

Consider the term $\left(\frac{W_s}{G}\right) \frac{\rho_G}{\rho_s}$

The maximum value of this term is $22.8 \times \frac{.0368}{131} = 0.0064 << 1$

Hence equation (11) reduces to $(-r_A) = \frac{F_{Ao}\, X_A}{\left(\frac{W_s}{G}\right) \rho_G\, V}$ (12)

The relative error will be calculated for the smallest rate measured, i.e., 0.027 lb.-moles/hr. lb. catalyst (data point 4, App. 1).

For this rate: $F_{Ao} = 8.02 \times 10^{-3}$ lb.-moles/hr.

$(W_s/G) = 22.8$

$X_A = 0.092$

The relative error of each variable in equation (12) must be considered:

(a) F_{Ao}: Flow measurement with a rotameter gives $\pm$ 2% error at full scale. This measurement was made at 25% of full scale. Therefore, relative error = $\pm$ 8%

absolute error = $\pm$ 0.6 x 10^{-3}

(b) x_A:

$$x_A = \frac{\text{gm.-moles OTA/gm. sample}}{\text{lb.-moles OX/lb. feed}}$$

Numerator: relative error = $\pm$ 1% (chromatograph sampling and analysis)

absolute error = $\pm$ 0.004 x 10^{-4}

Denominator: absolute error = 3.71 x 10^{-4} $(\frac{0.60}{8.02} + \frac{0.47}{20}) = \pm 0.36 \times 10^{-4}$

(0.60: OX Feed; 0.47: Air Feed)

Therefore, absolute error in conversion measurement

$$= 0.092 \left(\frac{0.004}{0.398} + \frac{0.36}{3.71}\right) = 0.009$$

(c) (W_s/G):

W_s: relative error has been arbitrarily taken as $\pm$ 2%

This should be ample because the catalyst was observed to be extremely free-flowing and no fluctuations in solids feeder speed could be observed.

Absolute error = 492 x 0.02 = $\pm$ 10 lb./hr.

G: relative error = $\pm$ 2.2% (rotameter at 90% scale)

absolute error = 21.6 x 0.022 = $\pm$ 0.47

(W_s/G): relative error = $\frac{10}{492} + \frac{.47}{20} = \pm 0.0424$

absolute error = $22.8 \times 0.0424 = \pm 0.97$

The relative error in the reaction rate is calculated by adding the relative errors of the variables in equation (12).

$$\text{Relative Error in Rate} = \frac{0.6}{8.02} + \frac{0.009}{0.092} + \frac{0.97}{22.8} = 0.20$$

Therefore, the measured reaction rate could vary by $\pm$ 20% because of experimental error.

APPENDIX 4

EQUIPMENT SPECIFICATIONS

Air Filters (No. 2 on Figure 1)

Type: Norgren Manual Drain Filter Type 12-002

Filter Screens: #1 - 75 microns

#2 - 25 microns

Orifice Plate (No. 3 on Figure 1)

Material: 0.125" 316 Stainless Steel plate

Plate Diameter: 1.245"

Orifice Diameter: 0.177" (#16 drill)

Throat Thickness: 0.0136"

Location of Pressure Taps: 1" from front and back face of orifice plate

Transmitter (No. 4 on Figure 1)

Manufacturer: Minneapolis Honeywell

Model: Design N7 Differential Converter with Non-Bleed Pilot Relay

Model No.: Y228N5G3-X-IV

Serial No.: 644053

Differential Pressure Range: 0 - 100" H_2O

Air Flow Controller (No. 5 on Figure 1)

Manufacturer: United States Gauge

Type: 11D

Serial No.: P7880

Range of Output Pressure: 3 - 15 psig

Air Control Valve (No. 6 on Figure 1)

Manufacturer: Research Controls Inc.

Type: 75S

Serial No.: 14037

Size: 1/2" NPT

Trim: G

Range: 3 - 15 psig

Action: air to open

Air Rotameter (No. 7 on Figure 1)

Manufacturer: Fischer and Porter (Canada) Ltd.

Serial No.: 64-10-B-1325/1

Tube: FP-1/2"-27-G-10

Float: 1/2"-GSVT-44 (316 S.S.)

Inlet and Outlet Connections: 1/2" N.P.T.

Air Preheater (No. 8 on Figure 1)

Manufacturer: American Standard Products Limited

Model: Ross Type 200-8 SSCF Shell and Tube Heat Exchanger

Heat Transfer Surface: 1.2 sq. ft.

Tube Material: stainless steel

No. of Passes: 1

O-Xylene Control Valve (No. 11 on Figure 1)

Manufacturer: Millaflow Corporation

Type: Diaphragm

Model No.: 41100000

O-Xylene Rotameter (No. 12 on Figure 1)

Manufacturer: Fischer and Porter (Canada) Ltd.

Tube: FP-1/8-16-G-5/81

Float: 1/8 - SA

Carburetor and Preheater Heating Elements

(1 unit on carburetor; 2 units on preheater)

Manufacturer: The Kanthal Corporation

Type: Kanthal A-1 strip 3/8" wide x 0.025" thick

Resistance: 0.073 ohms/ft. at 68°F

Total Resistance: 0.384 ohms/unit

Max. Voltage: 24 volts

Max. Power Input: 1500 watts/unit

Auxiliary Air Rotameter

Manufacturer: Fischer and Porter (Canada) Ltd.

Tube: FP-1/4-25-G-5/81

Float: 1/4 S.S.

Solids Feeder Heaters

Manufacturer: The Canadian Chromalox Company Limited

Cat. No.: T1-1848

Material: Copper Sheath

Type: Tubular Element bent into a U

Dimensions: Radius of Bend: 1 1/8"

Length of leg: 3 3/4"

Power Consumption: 750 watts @ 115 volts

Maximum Voltage: 115 volts

Coupling Between Solids Feeder and Drive

Supplier: Vickers-Warnick Ltd.

Type: Dalton ROSDC Rigid Coupling Torque Limiter

Range of Torque Adjustment: 0 - 35 ft.-lb.

Variable Speed Drive for Solids Feeder

Manufacturer: The Zero-Max Company

Model No.: E1-S6-M2

Speed Range: 0 - 50 RPM

Torque Rating: 85 inch-pounds

Solids Hold-up Tank Heaters

Manufacturer: The Kanthal Corporation

Material: Kanthal A-1 strip. Heater consists of six strips each 3/8" wide x 0.025" thick x 9' long

Configuration: Two strips connected in parallel and operated from one variable transformer. Thus, there are three independently controlled heating units.

Equivalent Resistance of Each Unit: 0.340Ω @ 68°F

Max. Power Consumption: 1700 watts/unit. 5100 watts total

Voltage Range: 0 - 24 volts

Salt Tank Immersion Heaters (No. 19 on Figure 1)

Manufacturer: The Canadian Chromalox Company Limited

Cat. No.: MTS-330-WSLM

Material: heater element: inconel sheath

threaded base: type 347 S.S.

Heated Length: 9"

Power Consumption: 1100 watts @ 230 volts

Max. Voltage: 230 volts

Power Regulation for Salt Tank Heaters

Manufacturer: The American Superior Electric Company Ltd.

Type: 117-T3 Powerstat Variable Transformer

Number of Units: 2. Each unit controls three salt tank heaters - one heater from each phase.

Connection: 3-Phase Wye

Primary Voltage: 240 volts, 3 phase

Output Voltage: 0 - 240 volts per phase

Max. Amps: 10

Max. KVA: 5.4 per unit

Salt Circulation Pump (No. 18 on Figure 1)

Manufacturer: Canada Pumps Ltd.

Type: 1 1/4" Class COV-c Vertical Cantilever Pump

Serial No.: 65-D-449

Rating: 5 USGPM

Head: 20 feet

RPM: 1150

Material: Steel

Drive: 1 H.P. Century Squirrel Cage Polyphase Induction Motor

Model No.: FVA9-305673

Serial No.: 2E520

Power: 230 volts, 3 phase, 60 cycle, 3.2 amps

Gas-Sampling Valve

Manufacturer: Carle Instruments, Inc.

Type: Micro-Volume Switching Valve With Zero Dead Volume

Cat. No.: 2014

Nominal Volume of Matched Loops: 1.0 ml.

Heater: Nichrome wire imbedded in Hiloset cement

Max. Heat Input: 60 watts @ 110 volts

Gas Chromatograph

Manufacturer: Beckman Instruments Inc.

Model: GC-2A With Thermal Conductivity Detector

Cat. No.: 17302

Serial No.: 213569

Recorder: Fisher Integrating Recorder

Serial No.: PWS 1803

Span: 0 - 1 m.v.

Response Time: 0.5 sec.

Thermocouple Wire

Manufacturer: Thermo Electric (Canada) Ltd.

Type: 1/16" Ceramo Thermocouple Wire

Identification No.: Chromel-Alumel: CES 16-116-CT

Platinum-Platinum 10% Rhodium: CES 16-116-P10

Copper-Constantan: CES 04-116-DT

Lead Wire: Chromel-Alumel: Type NN 24 CT

Platinum-Platinum 10% Rhodium: Type GG-24-PR

Copper-Constantan: Type NN-24-DT

Sight Glasses

Manufacturer: Swift Lubricator Company

Material: Vycor Glass

Size: 3/4" diameter x 1/4" thick

Heat Transfer Cement

Manufacturer: Thermom Manufacturing Company

Type: High Temperature Heat Transfer Cement

Grade: T-63

Refractory Cement

Manufacturer: Kaiser Refractories Company

Type: Hiloset Fire Brick Mortar

Insulating Materials

(a) Johns-Mannville Thermobestos Insulation

(b) Johns-Mannville No. 450 Insulating Cement

(c) Fiberglas Aerocor Insulation (for applications up to 400°F)

Heat Transfer Salt

Manufacturer: E. I. DuPont De Nemours & Co. (Inc.)

Type: Hitec Heat Transfer Salt

Melting Point: 288°F

Composition: Potassium Nitrate - 53%

Sodium Nitrite - 40%

Sodium Nitrate - 7%

Filters (located in the pressure taps and in the sample line)

Manufacturer: Gelman Instrument Company

Filter Holder: 1" S.S. Cat. No. 2113

Filter: Type A Glass Fiber

Temperature Recorders

1. Philips 12 point Continuous Recorder With Automatic Compensator

   Type PR 3210A/00

2. Two Minneapolis-Honeywell 12 point Recorders

   Model No.: Y15303846-12-(99)-0-000-(060)-11-060-(999)

   Serial No.: L 4681926002

   L 4681926001